Bioorganic Chemistry 91 (2019) 103147

Contents lists available at ScienceDirect

Bioorganic Chemistry

journal homepage: www.elsevier.com/locate/bioorg

Ugi efficient synthesis, biological evaluation and molecular docking of coumarin-quinoline hybrids as apoptotic agents through mitochondria-related pathways

Salman Taheri[a], Maryam Nazifi[a], Mahboubeh Mansourian[b,c,*], Leila Hosseinzadeh[d,*], Yalda Shokoohinia[d,e]

[a] Chemistry & Chemical Engineering Research Center of Iran, P.O. Box 14335-186, Tehran, Iran
[b] Medicinal Plants Research Center, Yasuj University of Medical Sciences, Yasuj, Iran
[c] Department of Pharmacology, Faculty of Medicine, Yasuj University of Medical Sciences, Yasuj, Iran
[d] Pharmaceutical Sciences Research Center, School of Pharmacy, Kermanshah University of Medical Sciences, Kermanshah, Iran
[e] Ric Scalzo Botanical Research Institute, Southwest College of Naturopathic Medicine, Tempe, AZ, USA

ARTICLE INFO

Keywords:
Coumarin-quinoline hybrids
Apoptosis
Mitochondria-related pathways
Bcl-2
Survivin
Cancer

ABSTRACT

Ugi reaction was a reliable procedure for the synthesis of new coumarin-quinoline frameworks. Excellent yields, mild reaction conditions and easily available and inexpensive starting materials are advantages of this protocol. Cytotoxic effects of fourteen products were investigated in A2780 human ovarian cancer cells. Two synthesized compounds (**L11** and **L12**) exhibited more anti-cancer activity than other derivatives with IC_{50} values of 0.042 mmol/L and 0.102 mmol/L, respectively and were thus selected for further studies. Apoptosis was induced through the intrinsic pathway by activating caspase 9 and ended at the executioner pathway of caspase 3. Measurement of intracellular reactive oxygen species (ROS) and mitochondrial membrane potential (MMP) were also carried out for both of them. Further studies on a mechanism by Real Time-PCR and Western blot analysis were performed for anti-apoptotic proteins Bcl-2 and survivin both in mRNA and protein level relating to the untreated A2780 cells. The treatment of A2780 cells with compound **L11** significantly (P-value ≤ 0.05) induced apoptosis by down-regulation of Bcl-2 and survivin both in mRNA and protein level via a single dose (0.042 mmol/L), as well as activation of caspase 9 and 3, loss of MMP, and high ROS. Accordingly, findings supported the first report under which the pro-apoptotic activity of compound **L11** as an apoptosis-inducing agent was related to mitochondrial-mediated dysfunction signaling pathways. Molecular docking supports experimental outcomes. Evidently, coumarin-quinoline scaffolds are potentially favorable options for further assessment as influential chemotherapeutic agents for the future.

1. Introduction

Cancer as a global health problem has progressed dramatically in recent years, likely to reach more than 13.1 million deaths by 2030 [1,2]. Ovarian cancer is a leading gynecologic malignancy. Cisplatin-based chemotherapy is the mainstay for treatment after surgical intervention of the ovarian cancer. The occurrence of chemo-resistance is a major challenge for fighting ovarian cancer [3,4].

Finding high-quality compounds is an important task in the step-by-step development of multi-target drug discovery (MTDD). This strategy only uses a chemical compound against the multi-target activity. This useful strategy in pharmaceutical chemistry is a way to reduce the likelihood of drug resistance, toxicity, difficulty dosage, drug interactions problems, or increase the patient satisfaction to exhibit more favorable pharmacokinetics and pharmacodynamics [5,6]. A hybrid molecule with the participation of two groups (or more) of pharmacophores in a molecular structure may form a new single multifunctional entity. The connection of multi-target drugs is challenging whilst being an opportunity and innovative to moderate numerous directed activities against numerous single receptors to create competent synergistic impact or in the form of dual behaving drugs [7]. The use of a wide range of information obtained from bioinformatics, structural biology, chemistry and pharmacology can be useful for discovering/designing and synthesizing new hybrid molecules with diverse bioavailability [5,8].

* Corresponding authors at: Medicinal Plants Research Center, Yasuj University of Medical Sciences, Yasuj, Iran (M. Mansourian); Pharmaceutical Sciences Research Center, School of Pharmacy, Kermanshah University of Medical Sciences, Kermanshah, Iran (L. Hosseinzadeh).
E-mail addresses: m.mansourian@yums.ac.ir (M. Mansourian), lhosseinzadeh90@yahoo.com (L. Hosseinzadeh).

https://doi.org/10.1016/j.bioorg.2019.103147
Received 30 March 2019; Received in revised form 20 July 2019; Accepted 22 July 2019
Available online 27 July 2019

Table 1
Formation of diamide Ugi reaction compounds (**L1-L14**).

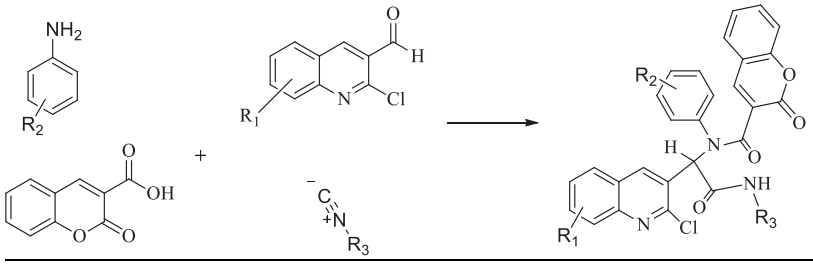

Product	R_1	R_2	R_3	Yield (%)[a]	RT[d]	Area (%)[e]
L1	H	H	C_6H_{11}[b]	88	6.58	100.00
L2	H	p-CH_3	C_6H_{11}	75	7.38	95.47
L3	H	m-CH_3	C_6H_{11}	88	7.43	100.00
L4	7-Me	H	C_6H_{11}	85	7.65	97.35
L5	7-Me	p-CH_3	C_6H_{11}	79	8.80	100.00
L6	7-Me	m-CH_3	C_6H_{11}	74	8.43	100.00
L7	6-Me	p-CH_3	C_6H_{11}	75	9.18	100.00
L8	6-Me	H	C_6H_{11}	86	7.67	97.24
L9	5,8-Dimethyl	p-CH_3	C_6H_{11}	69	9.02	100.00
L10	6-Me	m-CH_3	C_6H_{11}	81	9.18	100.00
L11	5,8-Dimethyl	H	C_6H_{11}	88	10.90	96.63
L12	5,8-Dimethyl	m-CH_3	C_6H_{11}	90	12.47	95.98
L13	H	H	*t*-Bu[c]	78	5.63	97.11
L14	5,8-Dimethyl	H	*t*-Bu	81	8.75	100.00

[a] Isolated yield.
[b] Cyclohexyl isocyanide.
[c] Tert-butyl isocyanide.
[d] Retention Time (HPLC).
[e] Area Percent (HPLC).

A preferred method to synthesize of the desired products with maximum efficiency includes the fewest possible steps using commercial available and environmentally friendly starting materials [9]. One-pot multi-component reactions with ease of implementation protocols, no need for isolation of intermediates, and high-speed have gotten much attention for the construction of a wide type of organic scaffolds [10–12].

Hybrid anti-cancer drugs such as lapatinib and sunitinib have remarkable advantages over conventional anti-cancer drugs due to their improved pharmacodynamic profiles [8]. Further research is essential to gain a better understanding of anti-cancer activities of these hybrids which may lead to design of new therapies that may improve patients' survival. Coumarin-quinoline hybrids are derivatives with different mechanisms of action [6,8,13,14].

Among heterocyclic compounds, quinoline derivatives are pharmacologically important [8,15,16]. Quinoline is the core of several synthetic drug compounds, such as chloroquine, that is used as an antimalarial agent [17]. Quinoline derivatives have remarkable biological properties such as anti-tumor [13,16,18,19], in the breast cancer [13,18], cervical cancer [20], lung cancer [19,20], and pancreatic cancer [20]. Coumarin derivatives, on the other hand, have medical benefits such as anti-microbial [21], anti-tuberculosis [22], anti-inflammatory [23,24], anti-Alzheimer [14], anti-coagulants [25], anti-influenza [26], anti-HIV [27], and anti-cancer [7,23,28,29] activities [6,8]. Hybridizing the coumarin nucleus with other moieties has created new molecules with improved anti-cancer activity profiles [6,7,23,29]. Coupling of different coumarin derivatives with different type of heterocyclic compounds such as quinoline [14], triazole [30], chalcone [23], indole [29], triazine [27], and α-lipoic acid [24] has produced novel hybrid molecules [6]. Also, a molecular hybridization approach with quinoline, which is based on triazole [30], pyrazole–quinoline–pyridine [15], coumarin [14], triazine [31], and some miscellaneous structures play important roles in the development of novel molecules for the remedy of numerous multifactorial diseases [8].

Despite a great number of studies of cancers, precise mechanisms of drug resistance remained elusive. It is generally believed that chemotherapeutic drugs like cisplatin reduce cancer cells by inducing programmed cell death (apoptosis) [3]. One of the vital cellular procedures for multicellular organisms' development and homeostasis is apoptosis [32]. During apoptosis, there are changes within cell morphology, namely membrane blebbing and the creation of apoptotic bodies as cell shrinkage, nuclear fragmentation, chromatin condensation, and DNA fragmentation. The regulation of apoptotic pathways has been investigated in numerous pharmaceutical studies [33–35]. Malignant disorders of the apoptotic process could directly or indirectly lead to many human diseases including cancer and neuro-degeneration such as Alzheimer's disease [32]. The inefficiency of apoptosis is a vital trait which permitting cancer cells to escape from death. Apoptotic signaling pathway activation is an anti-cancer drug target in cytotoxicity induction [13]. Apoptosis is regulated by the complex protein interaction networks which its phases are dependent on a subset of caspases (Cysteine-dependent ASPartyl specific proteASES) [33]. Human caspases with a clear role in apoptosis, are divided into two categories; the initiator caspases (caspase 2, 8, 9, and 10) and the effector caspases (caspase 3, 6, and 7) [36]. The outcome of every cell is eventually depended on the cross-talking of pro- or anti-apoptotic signaling pathways [37]. Anti-apoptotic B-cell lymphoma-2 (Bcl-2) family regulates mitochondria-mediated apoptosis pathways [34,35]. Overexpression of Bcl-2 in A2780 human ovarian cancer cells leads to the resistance to cisplatin and is associated with the tumor cell resistance to chemotherapeutic agents by preventing an apoptotic response [3,38,39]. Survivin cannot be traced within differentiated normal tissues whilst it exhibits overexpression within the majority of human neoplasms [40,41]. The expression of survivin at high levels is associated with more intense diseases, a reduction of tumor cell apoptosis, an increase of resistivity to chemotherapeutic agents and a shortened survival period [42]. Down-regulation of survivin, and the induction of

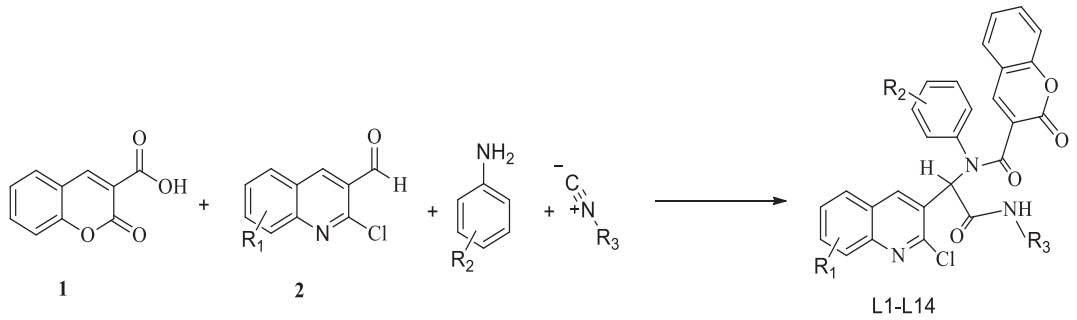

Scheme 1. Efficient synthesis of quinoline-coumarin scaffolds using an Ugi reaction.

apoptosis by activation of caspases 8, 9, and 3 are other effects of quinoline compounds [13,18,19], but no significant changes of Bcl-2 anti-apoptotic protein level were observed [13,19]. The use of a molecular hybridization strategy is highly suitable for introducing more potent molecules to simultaneously target more than a pathogenic mechanism [8].

Therefore, a series of hybrids with the coumarin-quinoline scaffolds as anti-cancer drug entities have been designed and synthesized based on Ugi reaction. It seems that the synthesized compounds, which have proper structures for the placement of pharmacophore groups in suitable spatial positions in enzymatic activities, may be useful for inhibiting activities of Bcl-2 and survivin toward inducing apoptosis. To this end, several important pathways of apoptosis were investigated. First, the screening and cytotoxic effects of hybrid compounds in the A2780 cancer cell line was performed for fourteen synthesized compounds (Table 1). The impact of the best compounds was measured on activities of caspase 9 and 3 as intrinsic and execution pathways, respectively. In addition, the production of intracellular reactive oxygen species (ROS) as well as mitochondrial membrane potential (MMP) were also evaluated as essential markers of apoptosis. Expression of survivin and Bcl-2 as key regulators of apoptosis were also evaluated both in gen and protein levels after cell treatment with the best compound by Real-time-PCR and the Western blot analysis. The results of theoretical and laboratory methods have accelerated the understanding of the interaction of molecules [43]. To achieve this goal in this project, a binding site of the best inducer of apoptosis on Bcl-2 and survivin was investigated by molecular docking along with the Western blot analysis.

2. Results and discussion

2.1. Chemistry

One of the most famous multi-component reactions is the Ugi four-component reaction which involves condensation of aldehydes, amines, isocyanides, and carboxylic acids [44]. Heterocyclic compounds play important roles in developing a new class of structural entities for pharmaceutical applications [6,8,29]. These compounds indicate diverse biological activities owing to their unique ability to copy structures of peptides and reversibly bind to proteins [29]. The present study aimed to combine the quinoline skeleton with the coumarin skeleton using alkyldiamide chains with different motifs to extract inhibitory potentials on anti-apoptotic proteins Bcl-2 and survivin (Table 1). In the present study, coumarin-3-carboxylic acid (2-oxo-2H-benzopyran-3-carboxylic acids) and 2-chloroquinoline 3- carbaldehyde used as raw materials in the presence of amines and isocyanide derivatives through a Ugi reaction.

A simple synthetic method developed for the efficient preparation of quinoline-coumarin derivatives using an Ugi four-component reaction involving coumarin-3-carboxylic acid, various derivatives of 2-chloroquinoline-3-carbaldehydes, cyclohexyl isocyanide and amines in methanol (see Scheme 1). All the synthesized compounds were fully characterized by FT-IR, ^{1}H NMR, and ^{13}C NMR spectral data (see Supplementary information S1). CHN elemental analysis was performed using an analysator Flash EA 1112 from Thermo Quest. The purities of compounds were confirmed by analytical high performance liquid chromatography (HPLC). Chromatograms were obtained using KNAUER on 18 reverse phase column (250 × 4.6 mm, Eurospher 100-5 C18) with water/acetonitrile (20:80 v/v) as solvent and the flow rate at 1.0 mL/min with UV detection at 257 nm (see Supplementary information S2).

2.2. Biological evaluation

2.2.1. Evaluation of the cytotoxic activity against A2780 cells by MTT assay

In the present study, cytotoxic effects of fourteen novel coumarin-quinoline structures on A2780 human cancer cells using 3-(4,5-dimethylthiazol-2-yl)-2,5-diphenyltetrazolium bromide (MTT) assay were investigated (see Supplementary information S3). In the MTT assay, doxorubicin was chosen as a positive control (see Supplementary information S4). It must be noted that doxorubicin has a potent antiproliferative effect against the growth of A2780 cells (IC_{50} = 6.1 μM). A2780 cells were treated with various concentrations of hybrids (0–100 μg/mL) for 24 h and the cell viability was evaluated by MTT growth inhibition assay. Compounds, **L11** and **L12**, were significantly more cytotoxic than other derivatives with IC_{50} values of 25 μg/mL (0.042 mmol/L) and 62 μg/mL (0.102 mmol/L), respectively and were thus selected for further studies (Fig. 1). In addition, the cytotoxic effect of the most potent compounds **L11** and **L12** were assayed in PC12 cells as a model of the normal cell (see Supplementary information S5). A glance at the Fig. S5 reveals that the **L11** and **L12** did not have any significant cytotoxic effect on the PC12 cells.

2.2.2. Caspase 9 and 3 activity assay

The induction of apoptosis is conducted through activation in

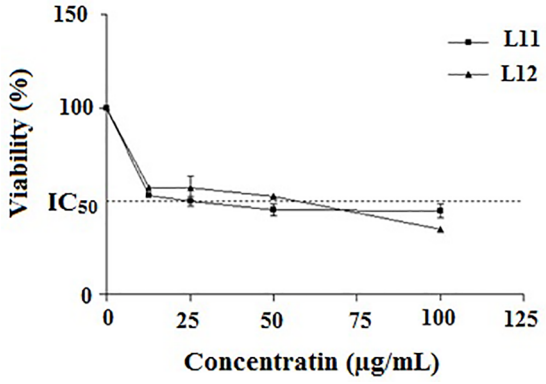

Fig. 1. Cytotoxic effects of **L11** and **L12** in A2780 cell line. The cytotoxic effect of the compounds was evaluated by MTT assay. Data presented as mean ± S.E.M (n = 3).

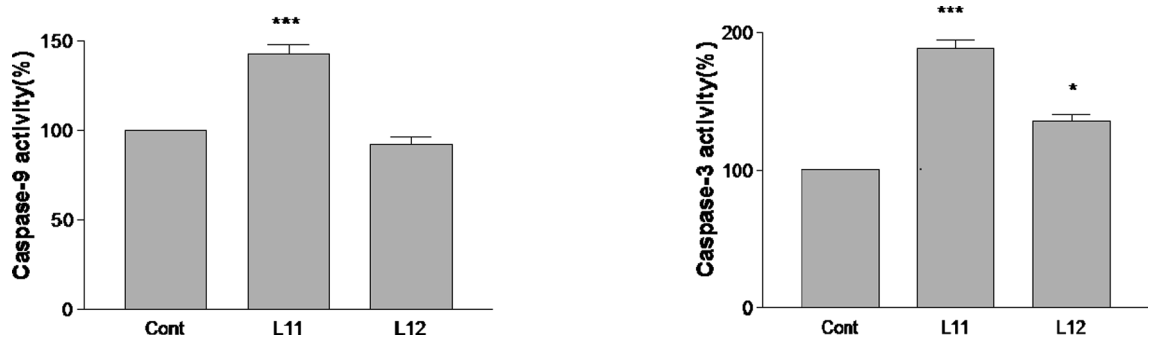

Fig. 2. Involvement of activation of caspases 9 and 3 in the induction of apoptosis by potent compounds on A2780 human ovarian cancer cells. Data presented as mean ± S.E.M. * P-value < 0.05, *** P-value < 0.001 vs. control.

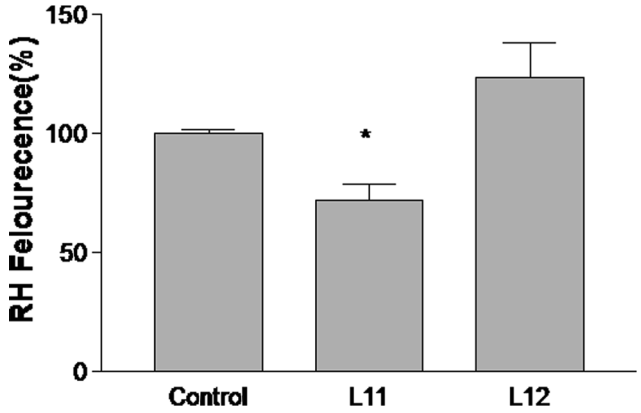

Fig. 3. The impact of compounds concerning mitochondrial membrane potential (MMP) collapse determined via Rhodamine 123. Data showed as mean ± S.E.M for three individual tests. **P-value < 0. 01 vs. control.

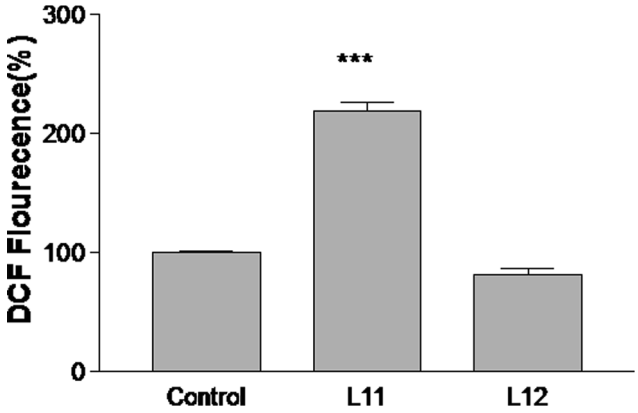

Fig. 4. The effect of potent compounds on the ROS generation in A2780 cell line. Data presented as the mean ± S.E.M of three separate experiments (n = 4). ***P-value < 0.001 vs. control.

reaction to various cell death stimulus through intrinsic (mitochondrial) and/or extrinsic (death receptor) pathways [13,35]. Activation of the intrinsic pathway as a response to a several stressing conditions, namely oxidative stress and DNA damage induced mitochondrial protein release e.g. cytochrome *c* (Cyt c) from intermembrane space into cytosol. Cyt c with other compounds e.g. ATP (or dATP) and Apaf-1 (apoptosis protease activating factor) creates a multimeric complex namely apoptosome which stimulates the activation of caspase 9. The stimulated caspase 9 activates and cleaves effector caspases e.g. caspase 7, 6 and 3 [13,40]. It is common knowledge that caspase 3 is the main executioner within the apoptotic procedure, and its stimulation causes cell death stages through proteolytic dismantling of extensive cellular components and pro-apoptotic factors' activation [35,45].

The results showed that compounds **L11** and **L12**, especially **L11**, dramatically increased the activity of caspase 3 in addition to cytotoxic effect in A2780 cells (Fig. 2). However, **L12** does not effect on the activity of caspase 9. Therefore, **L11**, a coumarin-quinoline hybrid, induced the cytotoxicity via activation of both caspase 9 and 3 in A2780 ovarian cancer cells in a single dose (at IC_{50} value 0.042 mmol/L) by more than 1.4–1.8 fold, following a 24 h treatment. It is indicated that the induction of apoptosis occurred via the intrinsic and execution pathways. The results were consistent with previous literature [13,28,31,35]. Manohar et al. synthesized novel molecular hybrids of 4-aminoquinoline and triazine as potential anti-cancer agents [31]. Among their synthesized products, two compounds had significantly activity against NCI 60 human tumor cell lines. Although, their representative compounds presented high activation of caspase 9, but none of them caused statistically significant activation of effector caspases 3 and 7 [31]. Furthermore, caspase 9 and 3 are prominent signaling proteins corresponding to the mitochondria-mediated apoptosis pathway [35].

2.2.3. Measurement of mitochondrial membrane potential

Mitochondrial function, a key parameter of cell health, can be assessed by monitoring changes in MMP [19]. As the cells' energy center, mitochondria are associated to cell apoptotic events. Mitochondrial dysfunction is a prominent apoptosis trait and includes procedures e.g. MMP reduction and mitochondrial permeability transition [19]. Changes in MMP in A2780 cells was detected for mitochondrial toxicity by evaluating the effects of **L11** and **L12** on MMP.

As shown in Fig. 3, after exposure to 0.042 mmol/L and 0.102 mmol/L of compounds **L11** and **L12** for 24 h, only **L11** notably showed lower fluorescence, and reduced the MMP of treated A2780 cells. Consistent with another study [19], compound **L11** induced the disturbance of MMP induced the apoptosis of A2780 cells through a mitochondria-mediated pathway. Amidst cancer cells' mediating apoptosis via mitochondrial pathway, the mitochondria discharged Cyt C within cytosol followed by apoptosis factors' induction and caspases activation [34,35].

2.2.4. Determination of intracellular reactive oxygen species level

ROS play the role of secondary messenger in regard to cellular signaling and associated to cell death and survival. Extreme ROS levels can lead to mitochondrial dysfunction and consequent cancer cells' apoptosis through mitochondrial dysfunction, MMP loss, Cyt C discharge, executioner caspases 3/9 cleavage and alterations in Bcl-2 family proteins levels [35]. The microscopic fluorescence imaging was conducted to evaluate whether compounds **L11** and **L12** induces ROS accumulation in A2780 cells. A2780 cells were incubated with IC_{50} concentrations of compounds, **L11** and **L12** (0.042 mmol/L and 0.102 mmol/L, respectively). It is evident from Fig. 4 that treatment using **L11** led to increased dihydrodichlorofluorescein (DCF) fluorescence intensity in comparison to control cells that were not subjected to

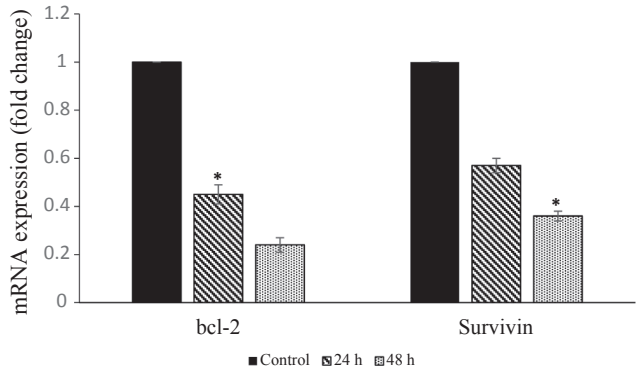

Fig. 5. Effects of compound **L11** on the Bcl-2 and survivin mRNA expression in A2780 cells with β-actin as a housekeeping control. The cells were treated with **L11** (0.042 mmol/L) and vehicle (Control group) for 24 and 48 h. Data represented as mean ± S.E.M; *P-value ≤ 0.05 statistically significant compared to control group.

treatment. Imaging evaluations showed that compound **L11** actively produced ROS and caused apoptosis induction in A2780 ovarian cancer cells through ROS-mediated mitochondrial dysfunction signaling pathway in the form of intrinsic routes. Based on the study conducted by Wang et al. [35], the aforementioned results indicated that compound **L11** stimulated the creation and aggregation of intracellular ROS within A2780 cells.

2.2.5. Assessment of Bcl-2 and survivin mRNA expression by Real-time-PCR

Caspases are regulated by many cellular processes. The suppression of caspase activity within tumor cells occurs in the presence of specific members of the Inhibitor of Apoptosis Proteins (IAP) protein family [33]. In other words, the IAPs as negative apoptosis regulator proteins endogenously antagonize the cell death by inhibiting enzymatic activities of mature caspases [46]. Furthermore, IAPs can also inhibit caspases 3 and 7 directly, and thus block downstream apoptotic events [3]. As the smallest IAPs member, survivin plays a prominent role in the inhibition of apoptosis and the division of cells. Survivin can be specific to terminal effector cell death protease, caspases 3 and 7 through BIR (Baculovirus IAP Repeat) domain causing hindrance in protease behavior and resulting apoptosis [40,47]. Survivin is verified as a cancer therapeutic target [48]. Researches imply that high survivin expression may enable it as a selective target carried via chemo-protective agents which induce apoptosis, namely within cancer cells. Hindered or decreased survivin expression alongside various cytotoxic agents may be useful for the treatment of cancer [40]. In addition, higher Bcl-2 expression levels within cancer cells stops apoptosis and causes tumor proliferation. Enhanced Bcl-2 expression is documented in numerous tumor cells of a drug-resistant nature [49].

Based on these results, in addition to Bcl-2, survivin as a member of the IAP family is over-expressed in A2780 cancer cells (Fig. 5). A2780 cells were treated at certain concentration of **L11** (0.042 mmol/L) and vehicle (Control group) for 24 h and 48 h for inhibition assessment of Bcl-2 and survivin mRNA level. The over-expression of Bcl-2 and survivin genes may contribute to the apoptotic inhibition in A2780 cells and the development of multidrug-resistance of human ovarian cancer [3,38–40]. The present data indicated that the expression of anti-apoptotic genes including Bcl-2 and survivin was significantly down-regulated after the treatment of A2780 cells with **L11** after 24 h and 48 h, respectively (P-value ≤ 0.05), while it was not significantly changed after 24 h for survivin in a time-independent manner. The decrement in mRNA levels of Bcl-2 and survivin, which were decreased due to the **L11** treatment in A2780 cells, indicated the sensitivity towards the **L11** treatment (Fig. 5), suggesting that Bcl-2 and survivin levels could regulate the caspase activation in A2780 cells. Therefore, the apoptosis induction was also confirmed at mRNA levels of Bcl-2 and survivin proteins.

In regard to numerous tumor cell lines, the existence of survivin is associated to apoptosis resistance which corresponds to malignancy enhancement [45,50]. In vitro researches showed the survivin hindrance increased or restored chemo-agents' cytotoxicity [45,51]. Animal researches exhibited profound effectiveness towards xenografts through adenoviral strategy targeted to survivin [45,52]. Despite the apoptosis inhibition nature of survivin and Bcl-2, they are active via different routes in cell apoptosis regulation. The mitochondrial pathways are mainly inhibited by the anti-apoptotic protein Bcl-2 [45,53], whilst survivin directly prevents and stimulation of processing of effector caspase 7 and 3 which typically act downstream of the signaling pathways [45,47] which implies the induction of cell apoptosis by compound **L11** via different pathways.

2.2.6. Western blot analysis

Anti-apoptotic proteins' expression that includes survivin and Bcl-2 upon A2780 cells' treatment via compound **L11** for a period of 48 h was conducted through Western blot analysis. The proteins' Bcl-2 family is an integral regulator concerning with an intrinsic apoptosis pathway. Such associated proteins share a minimum of one to four homologous areas named Bcl homology (BH) domains (BH1 to BH4) which regulate the competency of Bcl-2 proteins for the purpose of binding to one another to create hetero and homodimers. The BH domain is involved at numerous levels for the functioning of such proteins pertaining to cell survival and cell death [37,54]. The Bcl-2 protein is a member of the Bcl-2 family and is bonded to the external mitochondria surface as well as the surface of endoplasmic reticulum whilst separating pro-apoptotic members e.g. Bax from mitochondria and averts apoptotic death of cells [55]. Enhanced Bcl-2 expression is documented in numerous tumor cells of a drug-resistant nature [49].

In the present study, apoptosis-connected cellular processes were studied by the Western blot. Based on results, in addition to Bcl-2, survivin is over-expressed in A2780 cancer cells (Fig. 6). Changes in the protein expression of Bcl-2 and survivin (anti-apoptotic) was evaluated under the influence of compound **L11**. The A2780 cells, which were treated with a certain concentration (0.042 mmol/L) of **L11**, exhibited the widespread and effective induction of apoptosis after 48 h. As shown in Fig. 6, the immunoblot results confirmed that levels of Bcl-2 expression in cell line significantly (P-value ≤ 0.05) decreased by the treatment with compound **L11** compared to control cells (Fig. 6). Interestingly, the expression of survivin was also reduced in A2780 cells after the treatment with **L11** (P-value ≤ 0.05). Thus, it was found that compound **L11** inhibited Bcl-2 and survivin activities with the IC_{50} value of 0.042 mmol/L by the Western blot analysis.

L11 might intervene with the expression of survivin and Bcl-2 proteins or more likely activated degradation pathways of proteins. In regard to tumor cells, apoptosis may be activated through the stimulation of molecules that are upstream of apoptosis signaling or through the hindrance of anti-apoptotic parameters [13,35]. Researches on intrinsic apoptotic pathways showed that **L11** may induce intrinsic checkpoint protein caspase 9 whilst decreasing transcription level and the expression of anti-apoptotic Bcl-2 and survivin. The induction of apoptosis by **L11** was achieved by down- regulation of level expression of genes and proteins Bcl-2 and survivin, and activation of caspase 9 and 3.

On the other hand, our findings indicated that compound **L11** induced apoptosis by regulating Bcl-2, survivin, caspase 9 and 3, loss of MMP, and high ROS. The Bcl-2 protein is predominantly located on the mitochondria where the critical decision point, Cyt C release, is regulated. In regard to cancer cells, they inhibit the formation of a pore within the mitochondrial membrane and Cyt C discharge, thus preventing caspase 9 and 3 induction in downstream molecules [35]. According to prior suggestions, Bcl-2 protein expression reduction may cause MMP to collapse whilst accumulating intracellular ROS leads to

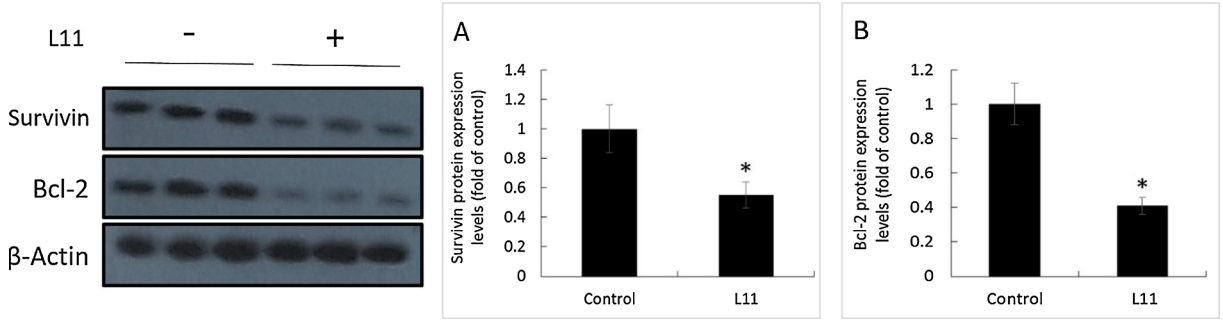

Fig. 6. Survivin and (B) Bcl-2 protein levels were assayed in cell lysates by Western blotting. Semi-quantitative data measured by imageJ software for survivin and Bcl-2 bands were normalized by the intensities of respective β-actin. *P-value ≤ 0.05 statistically significant compared to control group.

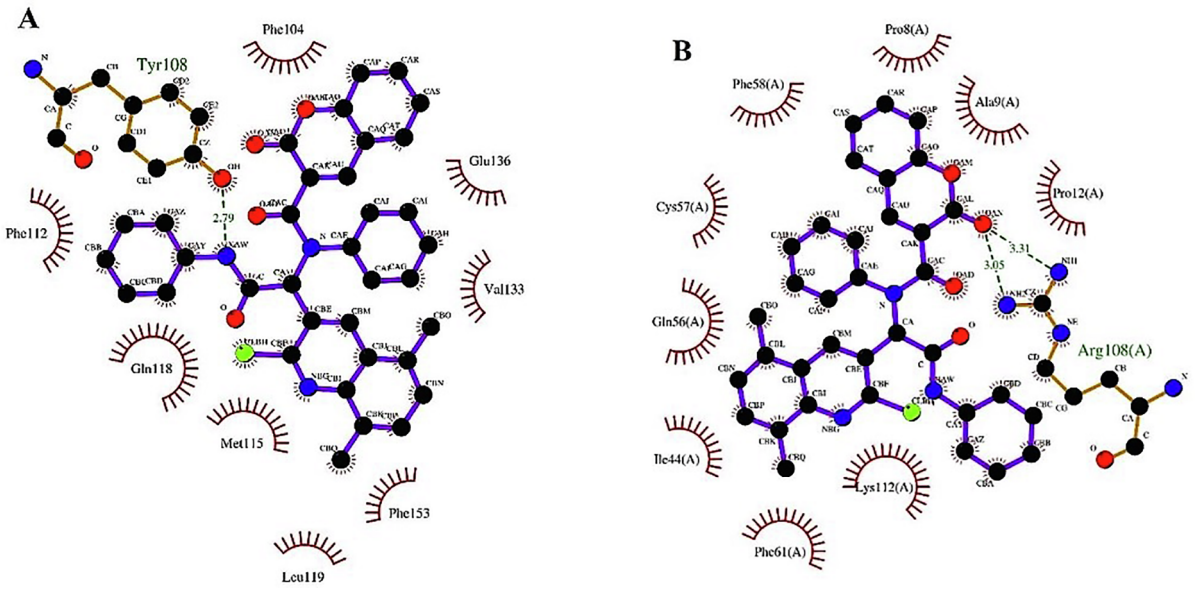

Fig. 7. Schematic interaction of the best docking resulting from AutoDock software presented by LigPlot software for (A) Bcl-2 and (B) Survivin. In this figure, compound **L11** exposure is blue-highlighted. Hydrogen bonding is in green and van der Waals interactions are in red circulars.

cell apoptosis through caspase 3 and 9 activation. The anti-proliferative impact of the compound **L11** was attributed to numerous processes, namely apoptosis activation and the expression of apoptosis-relevant proteins and genes. Consistent with other studies [19,35], the present results supported that the apoptosis induction in A2780 cancer cells by compound **L11** was related to mitochondrial dysfunction signaling pathways as an intrinsic pathway.

2.2.7. Molecular docking studies

The hybrid molecules have multiple biological activities, different or dual modes of action, modified selectivity profile, and reduced unfavorable side effects due to an involvement of pharmacophores in a molecular scaffold [5,6]. According to bioinformatics studies on possible pathways of apoptosis induction, in the present project attempts to determine the theoretical binding site and the binding energy of compound **L11** on Bcl-2 and survivin by molecular docking along with Western blotting analysis.

IAPs such as survivin can bind to caspases which are essential proteins in apoptosis, and subsequently deactivate their activity. After the apoptotic stimulus, Second Mitochondria-derived Activator of Caspases/Direct IAP-binding protein with low pI (Smac/DIABLO) protein as a deactivator for apoptosis inhibitors is released from the inner mitochondrial membrane into the cytosol, and thus endogenously antagonizes functions of the inhibitory activity of IAPs on caspases. Some synthetic compounds, which are called Smac-mimetics, can kill malignant cells by inhibiting IAPs. This specific binding of Smac-mimetics, as single agents, to IAPs cause caspases to be released from Smac, remove the IAP-mediated inhibition of caspases, thereby promoting apoptosis in a subset of human cancer cells [33,46,48,56]. The development of Smac-mimetics as novel anti-cancer drugs increases the utility, so that several compounds targeting IAPs are developed in clinical trials [56]. Analysis on molecular docking proved that survivin BIR domain binding to inhibitors may cause the discharge of caspases from survivin and bolster apoptosis as with prior documented results by others [40,46,57]. As an example, survivin blockers can conduct binding to survivin BIR domain within a common binding site such as Smac/DIABLO with sufficient energy for binding [40,46,57].

Starting from such conceptual design for further investigation of such hypothesis in parallel with biochemical studies about the apoptosis induction, molecular docking studies were conducted in details. Therefore, the evaluation of compound **L11** as a promising Smac-mimetic to BIR domain of survivin potentially was carried out via molecular docking. However, continued efforts to prove the ability of **L11** targeting both survivin and Bcl-2-regulated apoptosis as well as further in vitro studies should be conducted to provide more evidence on the anti-cancer effect of **L11** according to previous studies [4,7,29,40].

As shown in Fig. 7, some Bcl-2 amino acids including Phe104, Tyr108, Phe112, Met115, Gln118, Leu119, Val133, Glu136, and Phe153 are predicated to be within 4.0 Å of compound **L11** for forming intermolecular hydrophobic interactions. In addition, **L11** established a strong hydrogen bond with Tyr108 of Bcl-2 at a distance 2.79 Å. Based on **L11** inhibition constant (K_i = 401.24 nM), it is favorable to interact

with free binding energy −8.73 kcal/mol and electrostatic force −0.07 kcal/mol. Tyr108 and Gln118, Bcl-2 amino acids are typical residues which entail interaction with Bcl-2 blockers. It is noteworthy that Gln118 enables a robust interaction with BAX peptide [4,29]. As antagonists such as indole-coumarin hybrid small molecules were synthesized and designed as prospective molecules with targeting Bcl-2 due to their anti-cancer properties [7,29].

Based on estimated inhibition constant of **L11** (K_i = 1.40 μM) with the binding free energy (−7.98 kcal/mol), it is appropriate interaction with survivin. Hydrogen bonds adopt the role of stabilizers for ligand-protein interactions. A pair of hydrogen bonds with NH group of Arg108 and coumarin moiety oxygen carbonyl at distances 3.05 Å and 3.31 Å have vital responsibilities in survivin-**L11** complex stabilization as shown in Fig. 7. Electrostatic force between **L11** and survivin was −0.14 kcal/mol which entailed appropriate interaction concerning proteins and drugs [40]. It was reported that residues Pro8, Ala9, Pro12, Ile44, Gln56, Cys57, Phe58, phe61, and Lys112 of survivin were responsible for intermolecular hydrophobic interactions. Survivin protein possesses an individual *N*-terminal BIR domain from amino acids 15 to 89 as well as long C-terminal a-helix of amino acids 100 to 140 within its formation. Zinc ion in the survivin structure is placed at BIR domain center and has a vital role for BIR domain stabilization. Such domain is integral in inhibiting caspase behavior [41,47].

The predicted binding conformations revealed that compound **L11** had worthy inhibition potential with two electron donating groups (EDG) on quinoline ring without any substation on the aryl group and alkyldiamide chain. It was observed that the number of substituents and their respective positions on the aryl group and alkyldiamide chain also affected the orientation and binding pattern of compounds in the binding pocket of enzyme. The slight difference in potential was mainly affected by the position of substituent; and in some cases, the number of substituent also plays a role.

Findings from biochemical assays are in line with *in silico* docking researches for the prediction of potential anti-cancer behavior for such coumarin-quinoline hybrid. Docking researches present favorable information on compound **L11** binding affinity and aided in the understanding of interactions. Because of the high occurrence of unfavorable consequences activated through most present drugs, compound **L11** seems prospective to design enhanced selective therapeutic agents for the purpose of fighting cancer.

The findings of this study implied that novel coumarin-quinoline hybrids are prospective options for extended studies and may be presented as influential agents concerning chemotherapy. Extensive tests are required to analyze more detailed processes of compound **L11** activity. Additionally, it must be ascertained whether **L11** may also target other inhibitor apoptosis protein members, namely XIAP, cIAP2 and cIAP1 as well as other apoptosis-regulating proteins, namely Bcl-2 family that includes BAX or on other cell lines.

3. Conclusion

The present study introduced fourteen novel analogs of coumarin-quinoline hybrids with cytotoxic activity in the A2780 human ovarian cancer cells. Furthermore, **L11** and **L12** were introduced as the most active compounds compared with other compounds after evaluating its cytotoxic effects. Several methods were also performed including cell viability, induction of apoptosis, MMP assay, determination of intracellular ROS, caspase 9 and 3 activity assay. Since the applied compound **L11** in the present study had special biological properties, the expression of survivin and Bcl-2 as key regulators of apoptosis was also evaluated both at gen and protein levels after the cell treatment with compound **L11**. The molecular docking study was performed to understand the binding interaction of the most active analog.

The present study initially indicated that **L11** and **L12** as cytotoxic compounds could induce apoptosis in A2780 cell line. The synergistic effect of compound **L11** on apoptosis induction might be due to the regulation of anti-apoptotic agents including down-regulation of Bcl-2 and survivin and activation of caspase 9 and 3. Further examinations indicated that compound **L11** increased ROS levels, reduced MMP, and induced apoptosis in A2780 cells through the intrinsic mitochondrial pathway. Therefore, it was possible that a compound **L11** may be a sufficient agent in ovarian cancer therapy. The results can aid in designing novel synthetic coumarin-quinoline derivatives of competent cytotoxic behavior to induce apoptosis within A2780 cancer cells.

4. Experimental

4.1. Materials and methods

All reagents and chemical solvents in the present study were purchased from Merck, Fluka and Acros, and were used without any purification. Nuclear magnetic resonance (NMR) spectra were accomplished in $CDCl_3$ on Bruker AC 400 spectrometer operating at 500 MHz/125 MHz for ^{1}H NMR and ^{13}C NMR, respectively. Chemical shifts (δ) were reported in ppm, downfield from internal TMS standard. Precoated silica gel (E. Merck Kiesegel 60F254, layer thickness 0.25 mm) was applied for the thin layer chromatography (TLC).

4.2. Synthesize and characterization

4.2.1. Synthesis of coumarin-3-carboxylic acid (1)

In a round-bottomed flask, salicylaldehyde (10 mmol) and Meldrum's acid (12 mmol) in water (20 mL) were heated at reflux under stirring for 10 h. The reaction mixture was cooled and filtered on Büchner funnel. Further purification was done using the crystallization in ethyacetate. (Yield = 95%).

4.2.2. Synthesis of 2-chloroquinoline-3-carbaldehydes (2)

2-Chloroquinoline-3-carbaldehydes (**2**) were synthesized from acetanilides **1** via a Vilsmeier- Haack reaction (Scheme 2).

4.2.3. General procedure for the synthesis of chromene-3-carboxamide (L1–L14)

The reaction between 2-chloroquinoline-3-carbaldehydes and amine in methanol, imine was first created, and then coumarin-3-carboxylic acid was added to the reaction and stirring was continued for 30 min. Imine intermediate was prepared for attacking by the nucleophilic isocyanides. The resulting solution was stirred at room temperature for 4–6 h. The reaction was completed after 4–6 h. The reaction mixture was cooled and filtered on Büchner funne (Yields: 69–90%). Scheme 3 shows a mechanism for the synthesis of chromene-3-carboxamide.

4.2.3.1. N-(1-(2-chloroquinolin-3-yl)-2-(cyclohexylamino)-2-oxoethyl)-2-oxo-N-phenyl-2H-chromene-3-carboxamide (L1). White Solid, Yield: 88%. m.p: 199–202 °C. IR (KBr) (ν_{max}, cm^{-1}): 3280 (NH), 2930, 1728 (C=O), 1656 (C=O), 755; ^{1}H NMR)500 MHz, $CDCl_3$): δ_H:1.28–1.33 (m, 1H, CH), 1.39–1.64 (m, 4H, CH), 1.71–1.73 (m, 1H, CH), 1.82–1.84 (m, 1H, CH), 1.90–1.93 (m, 1H, CH), 2.08–2.10 (m, 1H, CH), 2.26–2.28(m, 1H, CH), 4.06–4.12 (m, 1H, CH), 6.93 (t, 1H, *J* = 10 Hz, Ar-H), 6.98–7.06 (m, 2H, Ar-H), 7.09 (s, 1H, Ar-H), 7.20 (brs, 2H, NH + Ar-H), 7.26 (d, 1H, *J* = 10 Hz, Ar-H), 7.34 (t, 1H, *J* = 5 Hz, Ar-H), 7.51 (t, 1H, *J* = 10 Hz, Ar-H), 7.56–7.59 (m, 2H, Ar-H), 7.70 (t, 2H, *J* = 5 Hz, Ar-H), 7.91 (d, 1H, *J* = 5 Hz, Ar-H), 8.05–8.09 (m, 2H, Ar-H), 8.10 (s, 1H, Ar-H). ^{13}C NMR (125 MHz, $CDCl_3$): δ_C: 25.4, 25.6, 25.8, 33.1, 33.6, 49.9, 62.6, 117.2, 118.3, 125.5, 126.1, 126.8, 127.1, 127.5, 128.34)2C), 128.39, 128.8, 129.1, 129.3, 131.3, 133.4, 138.3, 142.4, 143.4, 147.3, 151.3, 154.1, 159.1, 165.8, 167.0. Anal. Calcd. for $C_{33}H_{28}ClN_3O_4$: C, 70.02; H, 4.99; N, 7.42. **Found:** C, 70.42; H, 5.01; N, 7.63.

4.2.3.2. N-(1-(2-chloroquinolin-3-yl)-2-(cyclohexylamino)-2-oxoethyl)-2-oxo-N-(p-tolyl)-2H-chromene-3-carboxamide (L2). White Solid, Yield:

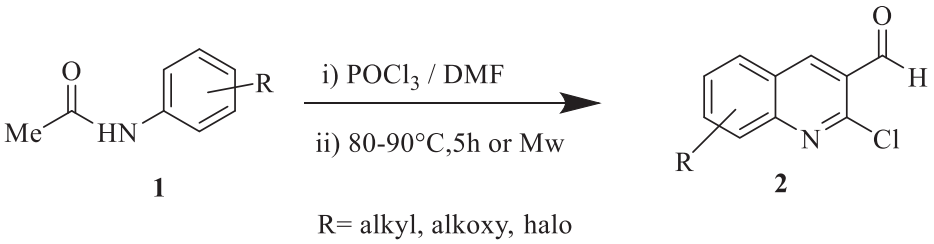

Scheme 2. Vilsmeier-Haak reaction.

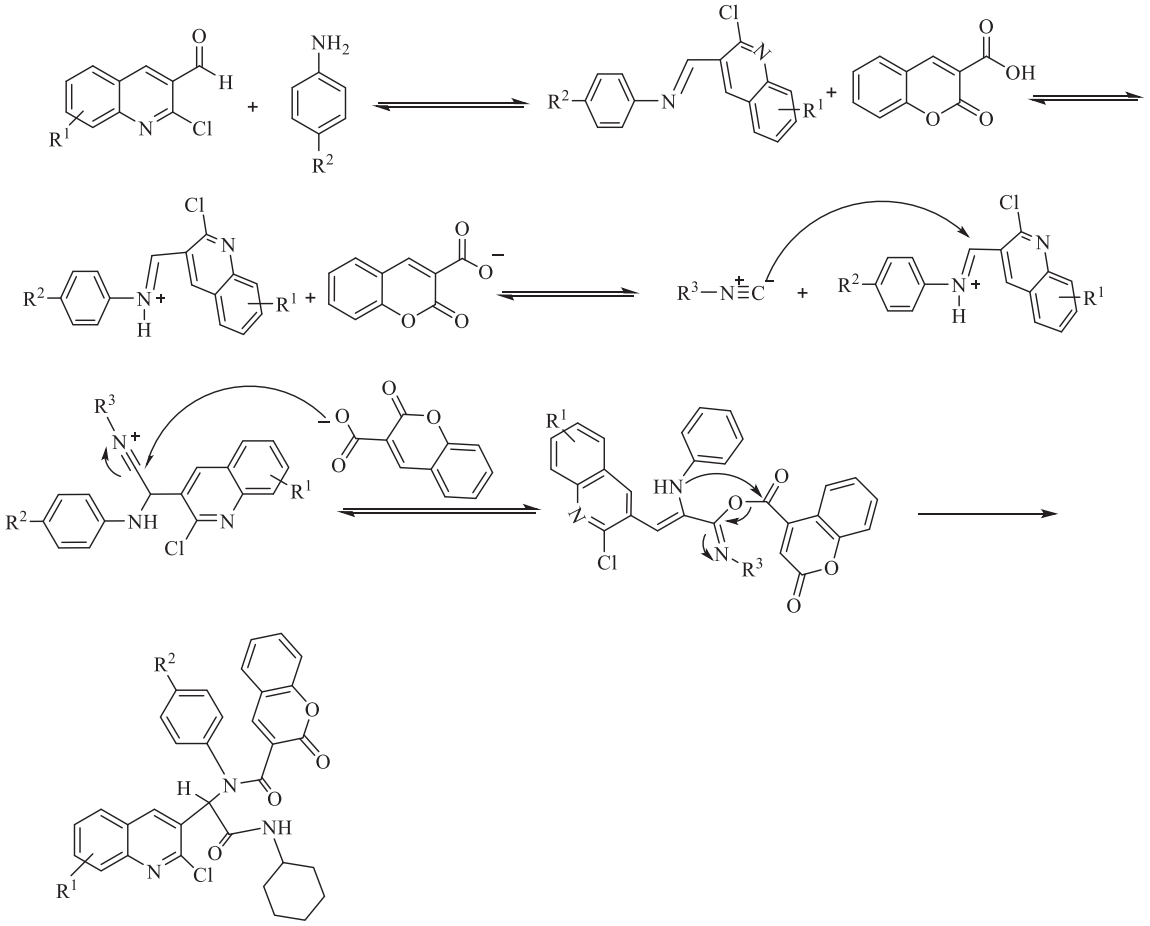

Scheme 3. Proposed mechanism for the synthesis of chromene-3-carboxamide.

75%. m.p: 251–255 °C. IR (KBr) (ν_{max}, cm^{-1}): 3292 (NH), 2930, 1735 (C═O), 1685 (C═O), 1656 (C═O), 750; ^{1}H NMR)500 MHz, $CDCl_3$): δ_H:1.15–1.26 (m, 1H, CH), 1.35–1.57 (m, 4H, CH), 1.66–1.68 (m, 1H, CH), 1.74–1.77 (m, 1H, CH), 1.85–1.88 (m, 1H, CH), 1.98)s, 3H, CH_3), 2.03–2.05 (m, 1H, CH), 2.16–2.20 (m, 1H, CH), 4.03–4.06 (m, 1H, CH), 6.72–6.74 (m, 2H, Ar-H), 6.95 (s, 1H, Ar-H), 7.03(brs, 1H, NH + CH), 7.21 (d, 1H, *J* = 5 Hz, Ar-H), 7.29 (t, 1H, *J* = 5 Hz, Ar-H), 7.46 (t, 1H, *J* = 10 Hz, Ar-H), 7.50–7.52 (m, 2H, Ar-H), 7.63–7.68 (m, 2H, Ar-H), 7.87 (d, 1H, *J* = 10 Hz, Ar-H), 7.97–8.05 (m, 2H, Ar-H), 8.08 (s, 1H, Ar-H).^{13}C NMR (125 MHz, $CDCl_3$): δ_C: 21.2, 25.4, 25.6, 25.8, 33.1, 33.6, 49.9, 62.6, 117.2, 118.4, 125.5, 126.2, 126.9, 127.0, 127.4, 128.4, 129.1, 129.8 (2C), 131.2, 133.2, 135.8, 138.7, 142.4, 143.2, 147.3, 151.4, 154.0, 159.1, 165.9, 167.1. Anal. Calcd. for $C_{34}H_{30}ClN_3O_4$: C, 70.40; H, 5.21; N, 7.24. **Found:** C, 70.83; H, 5.23; N, 7.49.

*4.2.3.3. N-(1-(2-chloroquinolin-3-yl)-2-(cyclohexylamino)-2-oxoethyl)-2-oxo-N-(m-tolyl)-2H-chromene-3-carboxamide **(L3)***. White Solid, Yield: 88%. m.p: 230–232 °C. IR (KBr) (ν_{max}, cm^{-1}):3279 (NH), 2928, 1723 (C═O), 1658 (C═O), 755; ^{1}H NMR)500 MHz, $CDCl_3$): δ_H:1.24–1.29 (m, 1H, CH), 1.37–1.59 (m, 4H, CH), 1.68–1.71 (m, 1H, CH), 1.80–1.82 (m, 1H, CH), 1.87–1.90 (m, 1H, CH), 2.03 (s, 3H, CH_3), 2.07–2.10 (m, 1H, CH), 2.22–2.31 (m, 1H, CH), 4.04–4.10 (m, 1H, CH), 6.71 (d, 1H, *J* = 5 Hz, Ar-H), 6.83–6.86 (m, 1H, Ar-H), 6.96 (s, 1H, Ar-H), 7.01 (brs, 2H, NH + OH), 7.24 (d, 1H, *J* = 10 Hz, Ar-H), 7.31 (t, 1H, *J* = 10 Hz, Ar-H), 7.48 (t, 1H, *J* = 10 Hz, Ar-H), 7.52–7.55 (m, 2H, Ar-H), 7.66–7.70 (m, 2H, Ar-H), 7.89 (d, 1H, *J* = 5 Hz, Ar-H), 7.95 (d, 1H, *J* = 10 Hz, Ar-H), 7.98 (s, 1H, Ar-H), 8.11 (s, 1H, Ar-H). ^{13}C NMR (125 MHz, $CDCl_3$): δ_C:21.4, 25.4, 25.6, 25.8 ,33.1, 33.6, 49.9, 62.7, 117.2, 118.4, 125.5, 126.2, 126.4, 126.9, 127.5, 128.31, 128.36, 128.8, 129.0, 129.5, 129.7, 131.3, 133.3, 135.8, 138.3, 139.1, 142.4, 143.1, 147.3, 151.4, 154.0, 159.1, 165.7, 167.0. Anal. Calcd. for $C_{34}H_{30}ClN_3O_4$: C, 70.40; H, 5.21; N, 7.24**. Found:** C, 70.84; H, 5.24; N, 7.51.

*4.2.3.4. N-(1-(2-chloro-7-methylquinolin-3-yl)-2-(cyclohexylamino)-2-oxoethyl)-2-oxo-N-phenyl-2H-chromene-3-carboxamide **(L4)***. White Solid, Yield: 85%. m.p: 225–226 °C. IR (KBr) (ν_{max}, cm^{-1}):3284 (NH), 2928, 1723 (C═O), 1652 (C═O), 757; ^{1}H NMR)500 MHz, $CDCl_3$):

δ_H:1.27–1.31 (m, 1H, CH), 1.35–1.59 (m, 3H, CH), 1.62–1.71 (m, 2H, CH), 1.80–1,82 (m, 1H, CH), 1.88–1.90 (m, 1H, CH), 2.05–2.08 (m, 1H, CH), 2.23–2.25 (m, 1H, CH), 2.51 (s, 3H, CH_3), 4.06–4.08 (m, 1H, CH), 6.91 (t, 1H, J = 5 Hz, Ar-H), 6.98–6.99 (m, 3H, Ar-H), 7.19 (brs, 1H, NH), 7.23 (d, 1H, J = 10 Hz, Ar-H), 7.29–7.32 (m, 3H, Ar-H), 7.53–7.57 (m, 3H, Ar-H), 7.66 (s, 1H, Ar-H), 7.94 (d, 1H, J = 5 Hz, Ar-H), 8.01 (d, 2H, J = 10 Hz, Ar-H). ^{13}C NMR (125 MHz, $CDCl_3$): δ_C: 22.3, 25.4, 25.6, 25.8, 33.1, 33.6, 49.9, 62.6, 117.2, 118.3, 124.9, 125.5, 125.8, 126.1, 127.4, 127.9 (2C), 128.8, 129.1, 129.4, 129.8, 133.3, 138.2, 138.7, 142.0, 143.3, 147.6, 151.3, 154.1, 159.1, 165.8, 167.1. Anal. Calcd. for $C_{34}H_{30}ClN_3O_4$: C, 70.40; H, 5.21; N, 7.24. **Found:** C, 70.85; H, 5.22; N, 7.48.

4.2.3.5. N-(1-(2-chloro-7-methylquinolin-3-yl)-2-(cyclohexylamino)-2-oxoethyl)-2-oxo-N-(p-tolyl-2H-chromene-3-carboxamide ***(L5)***. White Solid, Yield: 79%. m.p: 262–264 °C. IR (KBr) (ν_{max}, cm^{-1}):3269 (NH), 2929, 1722 (C=O), 1686 (C=O), 1644 (C=O), 758; ^{1}H NMR)500 MHz, $CDCl_3$): δ_H:1.26–1.31 (m, 1H, CH), 1.37–1.60 (m, 4H, CH), 1.68–1.71 (m, 1H, CH), 1.80–1.81 (m, 1H, CH), 1.88–1.90 (m, 1H, CH), 2.00 (s, 3H, CH_3), 2.05–2.07 (m, 1H, CH), 2.23–2.25 (m, 1H, CH), 2.50 (m, 3H, CH_3), 4.04–4.09 (m, 1H, CH), 6.76 (d, 2H, J = 10 Hz, Ar-H), 6.97 (s, 1H, Ar-H), 7.06 (brs, 2H, NH + Ar-H), 7.24 (d, 1H, J = 10 Hz, Ar-H), 7.30–7.32 (m, 2H, Ar-H), 7.53–7.54 (m, 2H, Ar-H), 7.58 (d, 1H, J = 10 Hz, Ar-H), 7.65 (s, 1H, Ar-H), 8.00 (s, 2H, Ar-H), 8.03 (s, 1H, Ar-H). ^{13}C NMR (125 MHz, $CDCl_3$): δ_C:21.2, 22.3, 25.4, 25.6, 25.8, 33.1, 33.6, 49.8, 62.6, 117.2, 118.4, 125.0, 125.5, 125.9, 126.3, 127.4, 127.9, 129.1, 129.72, 129.78 (2C), 133.2, 135.5, 138.7, 141.9, 142.0, 143.1, 147.6, 151.3, 154.0, 159.1, 165.9, 167.2. Anal. Calcd. for $C_{35}H_{32}ClN_3O_4$: C, 70.76; H, 5.43; N, 7.07. **Found:** C, 71.08; H, 5.45; N, 7.29.

4.2.3.6. N-(1-(2-chloro-7-methylquinolin-3-yl)-2-(cyclohexylamino)-2-oxoethyl)-2-oxo-N-(m-tolyl)-2H-chromene-3-carboxamide ***(L6)***. White Solid, Yield: 74%. m.p: 203–205 °C. IR (KBr) (ν_{max}, cm^{-1}):3282 (NH), 2929, 1738 (C=O), 1682 (C=O), 1661 (C=O), 747. ^{1}H NMR) 500 MHz, $CDCl_3$): δ_H:1.27–1.31 (m, 1H, CH), 1.36–1.60 (m, 4H, CH), 1.68–1.71 (m, 1H, CH), 1.80–1.82 (m, 1H, CH), 1.88–1.90 (m, 1H, CH), 2.04 (s, 3H, CH_3), 2.05–2.07 (m, 1H, CH), 2.22–2.25 (m, 1H, CH), 2.51 (s, 3H, CH_3), 4.06–4.08 (m, 1H, CH), 6.71 (d, 1H, J = 5 Hz, Ar-H), 6.80–6.84 (m, 1H, Ar-H), 6.96 (s, 2H, Ar-H), 7.02 (brs, 1H, NH), 7.24 (d, 1H, J = 5 Hz, Ar-H), 7.30–7.32 (m, 2H, Ar-H), 7.53–7.56 (m, 2H, Ar-H), 7.58 (d, 1H, J = 5 Hz, Ar-H), 7.66 (s, 1H, Ar-H), 7.95 (d, 1H, J = 5 Hz, Ar-H), 7.99 (s, 1H, Ar-H), 8.04 (s, 1H, Ar-H). ^{13}C NMR (125 MHz, $CDCl_3$): δ_C:21.4, 22.3, 25.4, 25.6, 25.8, 33.1, 33.6, 49.8, 62.7, 117.2, 118.4, 124.9, 125.5, 125.9, 126.2, 126.4, 127.4, 127.8, 128.8, 129.0, 129.5, 129.7, 131.3, 133.2, 138.2, 139.0, 142.01, 142.05, 143.1, 147.6, 151.3, 154.0, 159.1, 165.7, 167.1. Anal. Calcd. for $C_{36}H_{35}ClN_3O_4$: C, 70.76; H, 5.43; N, 7.07. **Found:** C, 71.39; H, 5.81; N, 7.12.

4.2.3.7. N-(1-(2-chloro-6-methylquinolin-3-yl)-2-(cyclohexylamino)-2-oxoethyl)-2-oxo-N-(p-tolyl)-2H-chromene-3-carbox Amide ***(L7)***. White Solid, Yield: 75%. m.p: 248–250 °C. IR (KBr) (ν_{max}, cm^{-1}):3282 (NH), 2929, 1738 (C=O), 1680 (C=O), 1661 (C=O), 747; ^{1}H NMR) 500 MHz, $CDCl_3$): δ_H:1.25–1.30 (m, 1H, CH), 1.36–1.58 (m, 4H, CH), 1.67–1.70 (m, 1H, CH), 1.79–1.81 (m, 1H, CH), 1.87–1.89 (m, 1H, CH), 1.99 (s, 3H, CH_3), 2.05–2.07 (m, 1H, CH), 2.22–2.24 (m, 1H, CH), 2.46 (s, 3H, CH_3), 4.03–4.09 (m, 1H, CH), 6.76 (d, 2H, J = 5 Hz, Ar-H), 6.94 (s, 1H, Ar-H), 7.07 (brs, 2H, NH + Ar-H), 7.22 (d, 1H, J = 5 Hz, Ar-H), 7.26–7.31 (m, 1H, Ar-H), 7.46–7.48 (m, 2H, Ar-H), 7.52 (t, 2H, J = 5 Hz, Ar-H), 7.76 (d, 1H, J = 5 Hz, Ar-H), 8.00 (d, 3H, J = 5 Hz, Ar-H). ^{13}C NMR (125 MHz, $CDCl_3$): δ_C: 21.2, 21.9, 25.4, 25.6, 25.8, 33.1, 33.6, 49.8, 62.6, 117.1, 118.4, 125.4, 126.2, 126.8, 126.9, 127.2, 127.9, 129.1, 129.7 (2C), 130.3, 133.2, 133.5, 135.5, 138.6, 141.6, 143.2, 145.9, 150.4, 154.0, 159.1, 165.9, 167.2. Anal. Calcd. for $C_{36}H_{35}ClN_3O_4$: C, 70.76; H, 5.43; N, 7.07. **Found:** C, 71.36; H, 5.82; N, 7.15.

4.2.3.8. N-(1-(2-chloro-6-methylquinolin-3-yl)-2-(cyclohexylamino)-2-oxoethyl)-2-oxo-N-phenyl-2H-chromene-3-carboxamide ***(L8)***. White Solid, Yield: 86%. m.p: 254–256 °C. IR (KBr) (ν_{max}, cm^{-1}): 3282 (NH), 2931, 1736 (C=O), 1682 (C=O), 1659 (C=O), 749; ^{1}H NMR) 500 MHz, $CDCl_3$): δ_H:1.25–1.30 (m, 1H, CH), 1.36–1.58 (m, 4H, CH), 1.68–1.70 (m, 1H, CH), 1.79–1.81 (m, 1H, CH), 1.87–1.89 (m, 1H, CH), 2.05–2.07 (m, 1H, CH), 2.22–2.25 (m, 1H, CH), 2.46 (s, 3H, CH_3), 4.03–4.09 (m, 1H, CH), 6.90 (t, 1H, J = 5 Hz, Ar-H), 6.97–6.99 (m, 3H, Ar-H + NH), 7.21 (d, 3H, J = 5 Hz, Ar-H), 7.28–7.31 (m, 1H, Ar-H), 7.44 (s, 1H, Ar-H), 7.47 (d, 1H, J = 5 Hz, Ar-H), 7.51–7.52 (m, 1H, Ar-H), 7.54 (d, 1H, J = 10 Hz, Ar-H), 7.75 (d, 1H, J = 5 Hz, Ar-H), 7.97–7.98 (d, 1H, J = 10 Hz, Ar-H), 8.01 (d, 2H, J = 5 Hz, Ar-H). ^{13}C NMR (125 MHz, $CDCl_3$): δ_C:21.9, 25.4, 25.6, 25.8, 33.1, 33.6, 49.9, 62.6, 117.2, 118.3, 125.5, 126.0, 126.7, 126.9, 127.1, 127.9, 128.8, 129.1, 129.4 (2C), 133.3, 133.6, 137.5, 138.3, 141.6, 143.3, 145.9, 150.4, 154.0, 159.1, 165.8, 167.1. Anal. Calcd. for $C_{34}H_{30}ClN_3O_4$: C, 70.40; H, 5.21; N, 7.24. **Found:** C, 70.83 H, 5.24; N, 7.43.

4.2.3.9. N-(1-(2-chloro-5,8-dimethylquinolin-3-yl)-2-(cyclohexylamino)-2-oxoethyl)-2-oxo-N-(p-tolyl)-2H-chromene-3-carboxamide ***(L9)***. White Solid, Yield: 69%. m.p: 292–294 °C. IR (KBr) (ν_{max}, cm^{-1}):3270 (NH), 2931, 1730 (C=O), 1651 (C=O), 759; ^{1}H NMR (500 MHz, $CDCl_3$): δ_H:1.26–1.31 (m, 1H, CH),1.37–1.43 (m, 2H, CH), 1.45–1.58 (m, 2H, CH), 1.68–1.75 (m, 1H, CH), 1.79–1.89 (m, 2H, CH), 2.05 (s, 3H, CH_3), 2.06–2.07 (m, 1H, CH), 2.20–2.23 (m, 1H, CH), 2.50 (s, 3H, CH_3), 2.66 (s, 3H, CH_3), 4.02–4.08 (m, 1H, CH), 6.80 (d, 2H, J = 5 Hz, Ar-H), 6.97 (s, 1H, Ar-H), 7.08 (brs, 2H, Ar-H + NH), 7.20 (d, 1H, J = 5 Hz, Ar-H), 7.24 (d, 1H, J = 5 Hz, Ar-H), 7.29–7.32 (m, 1H, Ar-H), 7.40 (d, 1H, J = 5 Hz, Ar-H), 7.52–7.55 (m, 2H, Ar-H), 7.67–7.69 (d, 1H, J = 5 Hz, Ar-H), 7.95 (s, 1H, Ar-H), 8.21 (s, 1H, Ar-H). ^{13}C NMR (125 MHz, $CDCl_3$): δ_C:18.0, 18.7, 21.2, 25.4, 25.5, 25.9, 33.0, 33.5, 49.8, 62.8, 117.2, 118.4, 125.4, 125.7, 126.3, 126.4, 127.5, 129.0, 129.3, 129.8, 131.0, 133.11, 133.18, 134.4, 135.8, 138.8, 139.2, 142.8, 147.1, 149.9, 154.1, 159.0, 165.9, 167.3. Anal. Calcd. for $C_{36}H_{34}ClN_3O_4$: C, 71.10; H, 5.64; N, 6.91. **Found:** C, 71.75; H, 6.01; N, 6.97.

4.2.3.10. N-(1-(2-chloro-6-methylquinolin-3-yl)-2-(cyclohexylamino)-2-oxoethyl)-2-oxo-N-(m-tolyl)-2H-chromene-3-carboxamide ***(L10)***. White Solid, Yield: 81%. m.p: 272–274 °C. IR (KBr) (ν_{max}, cm^{-1}):3290 (NH), 2931, 1738 (C=O), 1661 (C=O), 749; ^{1}H NMR (500 MHz, $CDCl_3$): δ_H:1.26–1.35 (m, 1H, CH), 1.37–1.41 (m, 2H, CH), 1.45–1.61 (m, 2H, CH), 1.68–1.71 (m, 1H, CH), 1.80–1.82 (m, 1H, CH), 1.88–1.90 (m, 1H, CH), 2.05 (s, 3H, CH_3), 2.06–2.07 (m, 1H, CH), 2.19–2.24 (m, 1H, CH), 2.48 (s, 3H, CH_3), 4.06–4.08 (m, 1H, CH), 6.72 (d, 1H, J = 5 Hz, Ar-H), 6.83–6.85 (m, 1H, Ar-H), 6.93 (s, 1H, Ar-H), 6.97–7.00 (brs, 1H, Ar-H), 7.03 (brs, 1H, N−H), 7.23 (d, 1H, J = 10 Hz, Ar-H), 7.30 (t, 1H, J = 5 Hz, Ar-H), 7.46 (s, 1H, Ar-H), 7.50 (d, 1H, J = 10 Hz, Ar-H), 7.54–7.55 (m, 2H, Ar-H), 7.78 (d, 1H, J = 5 Hz, Ar-H), 7.90 (d, 1H, J = 5 Hz ,Ar-H), 7.98 (s, 1H, Ar-H), 8.02 (s, 1H, Ar-H). ^{13}C NMR (125 MHz, $CDCl_3$): δ_C: 21.4, 21.9, 25.4, 25.6, 25.8, 33.1, 33.6, 49.8, 62.8, 117.2, 118.4, 125.5, 126.2, 126.4, 126.7, 126.9, 127.1, 127.9, 128.8, 129.0, 129.5, 129.8, 133.2, 133.6, 137.5, 138.3, 139.0, 141.7, 143.1, 145.9, 150.4, 154.0, 159.1, 165.7, 167.1. Anal. Calcd. for $C_{35}H_{32}ClN_3O_4$: C, 70.76; H, 5.43; N, 7.07. **Found:** C, 70.38; H, 5.81; N, 7.13.

4.2.3.11. N-(1-(2-chloro-5,8-dimethylquinolin-3-yl)-2-(cyclohexylamino)-2-oxo ethyl)-2-oxo-N-phenyl-2H-chromene-3-carboxamide ***(L11)***. White Solid, Yield: 88%. m.p: 273–275 °C. IR (KBr) (ν_{max}, cm^{-1}): 3261 (NH), 2930, 1724 (C=O), 1655 (C=O), 761; ^{1}H NMR (500 MHz, $CDCl_3$): δ_H: 1.26–1.35 (m, 1H, CH), 1.35–1.59 (m, 4H, CH), 1.68–1.73 (m, 1H, CH), 1.79–1.82 (m, 1H, CH), 1.87–1.89 (m, 1H, CH), 2.05–2.08 (m, 1H, CH), 2.20–2.24 (m, 1H, CH), 2.50 (s, 3H, CH_3), 2.66 (s, 3H, CH_3), 4.03–4.09 (m, 1H, CH), 6.94–7.03 (m, 4H, NH + Ar-H), 7.19 (d, 2H, J = 5 Hz, Ar-H), 7.24 (d, 2H, J = 10 Hz, Ar-H), 7.29–7.32 (m, 1H, Ar-H), 7.40 (d, 1H, J = 5 Hz, Ar-H), 7.52–7.56 (m, 2H, Ar-H), 7.66 (d,

1H, J = 5 Hz, Ar-H), 7.97 (s, 1H, Ar-H), 8.22 (s, 1H, Ar-H). ^{13}C NMR (125 MHz, $CDCl_3$): δ_C:18.0, 18.7, 25.4, 25.5, 25.9, 33.0, 33.5, 49.8, 62.8, 117.2, 118.3, 125.4, 125.6, 126.1, 126.4, 127.6, 128.9, 129.0, 129.1, 129.6, 131.1, 133.0, 133.2, 134.4, 138.5, 139.2, 143.0, 147.1, 149.8, 154.1, 159.0, 165.8, 167.3. Anal. Calcd. for $C_{35}H_{32}ClN_3O_4$: C, 70.76; H, 5.43; N, 7.07. **Found:** C, 71.11; H, 5.45; N, 7.25.

*4.2.3.12. N-(1-(2-chloro-5,8-dimethylquinolin-3-yl)-2-(cyclohexylamino)-2-oxoethyl)-2-oxo-N-(m-tolyl)-2H-chromene-3-carboxamide (**L12**)*. White Solid, Yield: 90%. m.p: 235–236 °C IR (KBr) (ν_{max}, cm^{-1}):3281 (NH), 2928, 1724 (C═O), 1657 (C═O), 762; ^{1}H NMR (500 MHz, $CDCl_3$): δ_H:1.25–1.28 (m, 1H, CH), 1.38–1.45 (m, 2H, CH), 1.48–1.56 (m, 2H, CH), 1.67–1.70 (m, 1H, CH), 1.79–1.88 (m, 2H, CH), 2.07 (s, 3H, CH_3), 2.08–2.10 (m, 1H, CH), 2.18–2.20 (m, 1H, CH), 2.50 (s, 3H, CH_3), 2.64 (s, 3H, CH_3), 4.03–4.07 (m, 1H, CH), 6.74 (d, 1H, J = 10 Hz, Ar-H), 6.85 (s, 1H, Ar-H), 6.96 (s, 2H, Ar-H), 7.09 (brs, 1H, N—H), 7.18 (d, 1H, J = 5 Hz, Ar-H), 7.23 (d, 1H, J = 5 Hz, Ar-H), 7.28–7.30 (m, 1H, Ar-H), 7.39 (d, 1H, J = 10 Hz, Ar-H), 7.51–7.53 (m, 2H, Ar-H), 7.68 (s, 1H, Ar-H), 7.96 (s, 1H, Ar-H), 8.22 (s, 1H, Ar-H). ^{13}C NMR (125 MHz, $CDCl_3$): δ_C:18.0, 18.7, 21.4, 25.4, 25.5, 25.8, 33.0, 33.5, 49.8, 62.9, 117.1, 118.4, 125.4, 125.7, 126.2, 126.3, 126.7, 127.6, 128.8, 129.0, 129.5, 129.8, 131.1, 132.9, 133.2, 134.4, 138.5, 139.0, 139.2, 142.9, 147.0, 149.9, 154.0, 159.0, 165.8, 167.3. Anal. Calcd. for $C_{36}H_{34}ClN_3O_4$: C, 71.10; H, 5.64; N, 6.91. **Found:** C, 71.52; H, 5.67; N, 7.17.

*4.2.3.13. N-(2-(tert-butylamino)-1-(2-chloroquinolin-3-yl)-2-oxoethyl)-2-oxo-N-phenyl-2H-chromene-3-carboxamide (**L13**)*. White Solid, Yield: 78%. m.p: 186–188 °C. IR (KBr) (ν_{max}, cm^{-1}): 3274 (NH), 2976, 1728 (C═O), 1664 (C═O), 758; ^{1}H NMR (500 MHz, $CDCl_3$): δ_H:1.56 (s, 9H, CH), 6.85 (s, 1H, Ar-H), 6.92 (t, 1H, J = 5 Hz, Ar-H), 6.98–6.99 (m, 2H, Ar-H), 7.18–7.30 (m, 4H, Ar-H + NH), 7.48–7.49 (m, 4H, Ar-H), 7.65 (t, 1H, J = 10 Hz, Ar-H), 7.70 (d, 1H, J = 10 Hz, Ar-H), 7.87 (d, 1H, J = 5 Hz, Ar-H), 7.95 (s, 1H, Ar-H), 8.16 (s, 1H, ArH). ^{13}C NMR (125 MHz, $CDCl_3$): δ_C: 29.1 (3 (CH_3)), 52.8, 62.8, 117.1, 118.3, 125.4, 125.9, 126.9, 127.0, 127.5, 128.2, 128.4, 128.8, 129.0, 129.1, 129.5, 131.4, 133.2, 138.5, 142.1, 143.1, 147.3, 151.3, 154.1, 158.6, 165.9, 167.3. Anal. Calcd. for $C_{31}H_{26}ClN_3O_4$: C, 68.95; H, 4.85; N, 7.78. **Found:** C, 69.41; H, 4.88, N, 7.95.

*4.2.3.14. N-(2-(tert-butylamino)-1-(2-chloro-5,8-dimethylquinolin-3-yl)-2-oxoethyl)-2-oxo-N-phenyl-2H-chromene-3-carboxamide (**L14**)*. White Solid, Yield: 81%. m.p: 180–182 °C. IR (KBr) (ν_{max}, cm^{-1}): 3340 (NH), 2925, 1716 (C═O), 1662 (C═O), 757; ^{1}H NMR (500 MHz, $CDCl_3$): δ_H:1.56 (s, 9H, CH), 2.51 (s, 3H, CH_3), 2.66 (s, 3H, CH_3), 6.82 (s, 1H, Ar-H), 6.97 (t, 1H, J = 5 Hz, Ar-H), 7.03 (t, 2H, J = 5 Hz, Ar-H), 7.15 (s, 1H, NH), 7.20–7.24 (m, 3H, Ar-H), 7.28–7.31 (m, 2H, Ar-H), 7.41 (d, 1H, J = 5 Hz, Ar-H), 7.50–7.54 (m, 2H, Ar-H), 7.92 (s, 1H, Ar-H), 8.29 (s, 1H, Ar-H). ^{13}C NMR (125 MHz, $CDCl_3$): δ_C: 18.0, 18.6, 29.0 (3 (CH_3)), 52.7 (2 (CH_3)), 63.3, 117.1, 118.3, 125.3, 125.8, 126.1, 126.4, 127.7, 128.9, 129.0, 129.1, 129.7, 131.2, 133.0, 133.1, 134.4, 138.8, 138.9, 142.8, 147.1, 149.8, 154.1, 158.6, 165.9, 167.6. Anal. Calcd. for $C_{33}H_{30}ClN_3O_4$: C, 69.77; H, 5.32; N, 7.40. **Found:** C, 70.19; H, 5.34, N, 7.64.

5. Biological studies

5.0.1. Antiproliferative activity

5.0.1.1. Cell culture

The aforementioned A2780 cells were subjected to culturing using Dulbecco's adjusted Eagle's medium (DMEM-F12) including 10% (v/v) fetal bovine serum (FBS), 100 U/mL penicillin and 100 mg/mL streptomycin. Upon 2 to 3 days, the medium was changed and subjected to sub-culturing as soon as the density of the cell population achieved 70–80% confluence.

5.0.1.2. Cell viability assay

MTT assay was performed on A2780 and PC12 cells in order to evaluate the cytotoxicity of compounds [29,38]. Doxorubicin was used as a positive control. Based on the manufacturer's protocol, the cells were cultured onto a 96-well cell culture plates at the density of 15,000 cells/well. After 24 h, various concentrations of compounds (0–100 μg/mL) were added to wells following by the incubation for 24 h. Subsequently, 20 μL of 5.0 mg/mL MTT solution was put into each well; and the cells were incubated for an additional 4 h. For the next stage, the medium was omitted prior to the dissolving of the purple formazan crystals within DMSO. An ELISA plate reader was used to determine the absorbance with test wavelength (570 nm) and reference wavelength (630 nm) to acquire simple signal i.e. OD570-OD630.

5.0.2. Caspase 9 and 3 activity assay

Caspase 9 and 3 activities were determined using the sigma colorimetric caspase kit. To this end, A2780 cells were seeded in a 12-well plate and incubated for 24 h. 0.042 mmol/L and 0.102 mmol/L of **L11** and **L12**, respectively were then added to wells and incubated for the next 24 h. Thereafter, the treated cells were centrifuged at 1200 rpm for 5 min and were lysed in 15 μL of the cell lysis buffer included with the kit. The extraction of protein content of cells was achieved by the centrifugation of lysates at 16,000–20,000 rpm and 4 °C for 15 min. The substrate reaction buffer containing caspase 3 substrate and caspase 9 substrate was added to the supernatant and then incubated for 2 h at 37 °C. The absorbance was then read at 405 nm by means of a plate reader (BioTek, H1M).

5.0.3. Measurement of mitochondrial membrane potential

For the current research, a cell penetrative dye i.e. rhodamine 123 fluorescent dye was utilized to monitoring MMP. MMP depolarization during cell apoptosis led to rhodamine 123 loss from mitochondria and reduced intracellular fluorescence intensity. To summarize, upon the final treatment stage, the cells received 5 mg/l rhodamine 123 for a period of 30 min at temperature 37 °C. Measurement of the fluorescent intensity was conducted at excitation wavelength (488 nm) and emission wavelength) 520 nm (using fluorescence micro-plate reader (BioTek, H1M, and USA).

5.0.4. Determination of intracellular reactive oxygen species level

Dihydrodichlorofluorescein diacetate (DCF-DA) as a non-fluorescent lipophilic ester was used to examine intercellular ROS level which effortlessly surpasses the plasma membrane and enters the cytosol where an unspecific esterase rapidly removes the acetate group. Green fluorescence is achieved upon this molecule's oxidation to fluorochrome DCF. The fluorescence intensity typically shows the extent of ROS presence. Upon a 24 h seeding period, a PBS buffer (PH 7.4) was used to wash the cells. The cells were then pretreated using selective compounds (0.042 mmol/L and 0.102 mmol/L of **L11** and **L12**, correspondingly) for a period of 24 h. Upon washing by PBS, the cells were subjected to incubation using 20 μL DCF-DA at a temperature of 37 °C for a period of 30 min. The DMSO in the solution was not higher than 0.5%. Upon incubation, Triton X-100 was used to lyse cells. The fluorescence was measured at excitation wavelength (488 nm) and emission wavelength (528 nm) by utilizing a fluorescence micro-plate reader (BioTek, H1M, USA).

5.0.5. Assessment of mRNA expression by Real-time-PCR

The total RNA extraction was done using RNA X Plus solution according the manufactured procedure. The purity and total concentration of mRNA were quantified by Nanodrop 1000 Spectrophotometer (Wilmington, USA) and qualified by electrophoresis in 1.1% agarose

gel. Prior to the gene expression assay, the reverse transcription of extracted RNA into cDNA carried out RevertAid First Strand cDNA Synthesis. The reaction was then running in MIC real time PCR machine (Bio Molecular System, Australia) using SYBR green (Prime Script RT Master Mix, Takara). The following primer sequences were used: Bcl-2: F: 5′-TTGTGGCCTTCTTTGAGTTCGGTG-3′ and R: 5′-GGTGCCGGTTCA GGT ACTCAGTCA-3′, survivin: F: 5′-ACCGCATCTCTACATTCAAG-3′ and R: 5′-CAAGTCTGGCTCGTTCTC-3′, and β-actin: F: 5′- GTGGACAT CCGCAAAGAC-3′; R: 5′-AAAGGGTGTAACGCAACTA-3′. Quantitative analysis of raw data was done by Pfaffl method; and β-actin was considered as a housekeeping gene.

5.0.6. Western blot experiments

For the purpose of determining survivin and Bcl-2 protein levels, the western blot analysis was conducted. The selected dose (IC_{50} value = 0.042 mmol/mL) of **L11** (treatment group) and vehicle (Control group) was used for cells' treatment for a period of 48 h. Cold PBS was used to wash harvested cells three times and cell lysates were acquired upon incubation using Invitrogen Life Technologies, USA cell extraction buffer as well as PMSF and protease inhibitor cocktail tablet, Roche, Germany for a period of 30 min. Cell debris were omitted from lysates via centrifugation at 13,000*g* for a period of 20 min. Protein concentrations of every specimen was ascertained via Lowry's approach. Proteins of equal quantities i.e. 40 μg were electrophoresed for a period of 3 h at 20 mA on SDS-PAGE and then electro-blotting took place to transfer them to PVDF membranes. 5% skimmed milk was used to inhibit the membrane for a period of 45 min under room temperature prior to being incubated with anti-Bcl-2 and anti-survivin antibodies (1:1000) within 1 TBS possessing 0.01% Tween-20 buffer left overnight at a temperature of 4 °C. A TBST-20 buffer was used to wash the membrane three times prior to incubation of secondary HRP-conjugated antibodies for a period of 1.5 h under room temperature. Western blotting luminol reagent, Santa Cruz technology was used to visualize the bands. ImageJ software, version 1.41 was used to conduct semi-quantitative analysis on the developed bands.

5.0.7. In silico simulation study

In silico calculations were conducted according to known literature-reported protocols [58,59]. The present study was conducted using the anti-apoptotic proteins Bcl-2 and survivin as targets (receptors) associated with apoptosis. The human sequence of subjected targets was obtained from NCBI (www.ncbi.nlm.nih.gov). The three-dimensional (3D) X-ray structure of human targets was used for docking downloaded from Protein Data Bank (PDB) (http://www.rcsb.org).

The Bcl-2 crystal structure within composite with BAX BH3 peptide (PDB ID: 2XA0) was chosen because of its minimal E-value i.e. 2.8e-98 at 100% sequence identity as the target. In regard to the stoichiometry, the Bcl-2 protein is monomeric and is a dimer of chains A and B. Every monomeric unit possesses ligand peptide BAX which is bound to the protein [4,29]. Survivin contains chains A and B and is a dimer protein. These chains have approximately similar amino acid pattern with chain B having two extra acids within the C terminal (Met, Asp) [40]. The chain A of survivin and Bcl-2 were chosen for the purpose of docking whilst the bound peptide was omitted from the Bcl-2 receptor active site [40,45].

The two-dimensional (2D) structure of compounds was drawn by ChemOffice 2015 and optimized using HyperChem 7.0 (Hypercube, Inc., Gainesville, FL, USA; http://www.hyper.com). Details of the optimization procedure were previously described [43,59]. Compound **L11** was docked into binding sites of receptors using AutoDock 4.2 [60]. Molecular docking studies were conducted for this ligand to obtain information on the binding energy and the ligand-protein interactions in details [58]. Docking was performed with the routine procedure of this software [60]. In the docking protocol, the ligand was assumed to be a flexible molecule to rotate all rotatable bonds of ligand to obtain the best and most optimal conformer of ligand within active sites of receptors.

Since the location of the binding site of ligand in the complex has been known by site-directed mutagenesis, the grid box was centered on the C_α atom of Gln118 of Bcl-2 at a resolution of 2.7 Å (2XA0) [61]; and on survivin at resolution of 2.71 Å (1E31) [62] at the coordinates X = −24.532, Y = 36.317, and Z = 64.94 [40]. Using the AutoGrid 4, the grid parameter file was set to grid box dimensions of 60 × 60 × 60. The grid point spacing was to 0.375 Å as the default value. A cluster analysis was performed at the end of docking experiment with 200 runs [58]. A Lamarckian genetic algorithm (LGA) program in the Autodock was used to calculate different ligand conformers [63]. The interaction binding energy was also calculated. Among various conformations of interactions between this compound and targets Bcl-2 and survivin, the conformation was selected with the best scored pose with the lowest binding energy (−8.73 and −8.08 kcal mol^{-1}, respectively). The resulting 2D poses were visually analysed to understand the interaction pattern by the LIGPLOT software [64].

Declaration of Competing Interest

The authors stated no conflict of interest.

Acknowledgement

A part of this project was financially supported by Medicinal Plants Research Center affiliated to Vice Chancellery for research, Yasuj University of Medical Sciences, Yasuj, Iran (Grant No. IR. YUMS.REC.1396.84). We are grateful to Dr Jon F. Parcher, National Center for Natural Products Research, University of Mississippi, MS, Oxford, USA for Native-English editing of the manuscript. The authors are appreciative to all members of Chemistry & Chemical Engineering Research Center of Iran, Tehran, Iran for synthesis of the compounds. We also thankful to the Pharmaceutical Sciences Research Center, School of Pharmacy, Kermanshah University of Medical Sciences, Kermanshah, Iran.

Appendix A. Supplementary material

Supplementary data to this article can be found online at https://doi.org/10.1016/j.bioorg.2019.103147.

References

[1] U.N.I.o. Health, Cancer trends progress report–2011/2012 update, Bethesda: National Cancer Institute, NIH, DHHS, Bethesda, MD, February 2019, https://progressreport.cancer.gov. 19, 2012.
[2] S. Mehrabi, H. Shirhzi, M. Rasti, Normal serum prostate specific antigen levels in men in Yasuj province, Islamic Republic of Iran, East Mediterr. Health J. 13 (5) (2007) 1190–1194.
[3] M. Singh, P. Chaudhry, F. Fabi, E. Asselin, Cisplatin-induced caspase activation mediates PTEN cleavage in ovarian cancer cells: a potential mechanism of chemoresistance, BMC Cancer 13 (1) (2013) 233.
[4] N. Nordin, M. Fadaeinasab, S. Mohan, N.M. Hashim, R. Othman, H. Karimian, V. Iman, N. Ramli, H.M. Ali, N.A. Majid, Pulchrin A, a new natural coumarin derivative of Enicosanthellum pulchrum, induces apoptosis in ovarian cancer cells via intrinsic pathway, PLoS ONE 11 (5) (2016) e0154023.
[5] A. Abdolmaleki, J.B. Ghasemi, Dual-acting of hybrid compounds-A new dawn in the discovery of multi-target drugs: lead generation approaches, Curr. Top. Med. Chem. 17 (9) (2017) 1096–1114.
[6] S. Sandhu, Y. Bansal, O. Silakari, G. Bansal, Coumarin hybrids as novel therapeutic agents, Bioorg. Med. Chem. 22 (15) (2014) 3806–3814.
[7] P.R. Kamath, D. Sunil, M.M. Joseph, A.A.A. Salam, T. Sreelekha, Indole-coumarin-thiadiazole hybrids: an appraisal of their MCF-7 cell growth inhibition, apoptotic, antimetastatic and computational Bcl-2 binding potential, Eur. J. Med. Chem. 136 (2017) 442–451.

[8] V. Abbot, P. Sharma, S. Dhiman, M.N. Noolvi, H.M. Patel, V. Bhardwaj, Small hybrid heteroaromatics: resourceful biological tools in cancer research, RSC Adv. 7 (45) (2017) 28313–28349.
[9] A. Dömling, I. Ugi, Multicomponent reactions with isocyanides, Angew. Chem. Int. Ed. Engl. 39 (18) (2000) 3168–3210.
[10] R.V. Orru, M. de Greef, Recent advances in solution-phase multicomponent methodology for the synthesis of heterocyclic compounds, Synthesis 2003 (10) (2003) 1471–1499.
[11] H. Bienaymé, C. Hulme, G. Oddon, P. Schmitt, Maximizing synthetic efficiency: Multi-component transformations lead the way, Chem. Eur. J. 6 (18) (2000) 3321–3329.
[12] A. Darehkordi, F. Zand-Vakili, A.T. Rafsanjani, A novel gabapentin based intermolecular Ugi four-center, three-component reaction for preparing N-cyclohexyl-2-(3-oxo-2-azaspiro [4, 5] decan-2-yl)-2-aryl acetamide derivatives, Tetrahedron Lett. 57 (4) (2016) 498–501.
[13] Y. Ding, T.A. Nguyen, PQ1, a quinoline derivative, induces apoptosis in T47D breast cancer cells through activation of caspase-8 and caspase-9, Apoptosis 18 (9) (2013) 1071–1082.
[14] Y. Duarte, A. Fonseca, M. Gutiérrez, F. Adasme-Carreño, C. Muñoz-Gutierrez, J. Alzate-Morales, L. Santana, E. Uriarte, R. Álvarez, M.J. Matos, Novel coumarin-quinoline hybrids: design of multitarget compounds for Alzheimer's disease, ChemistrySelect. 4 (2) (2019) 551–558.
[15] C.B. Sangani, J.A. Makawana, X. Zhang, S.B. Teraiya, L. Lin, H.-L. Zhu, Design, synthesis and molecular modeling of pyrazole–quinoline–pyridine hybrids as a new class of antimicrobial and anticancer agents, Eur. J. Med. Chem. 76 (2014) 549–557.
[16] S. Jain, V. Chandra, P.K. Jain, K. Pathak, D. Pathak, A. Vaidya, Comprehensive review on current developments of quinoline-based anticancer agents, Arab J Chem. (2016).
[17] A.R. Parhizgar, A. Tahghighi, Introducing new antimalarial analogues of chloroquine and amodiaquine: a narrative review, Iran J. Med. Sci. 42 (2) (2017) 115–128.
[18] J. Bernzweig, B. Heiniger, K. Prasain, J. Lu, D.H. Hua, T.A. Nguyen, Anti-breast cancer agents, quinolines, targeting gap junction, Med. Chem. 7 (5) (2011) 448–453.
[19] C.C. Chiu, H.L. Chou, B.H. Chen, K.F. Chang, C.H. Tseng, Y. Fong, T.F. Fu, H.W. Chang, C.Y. Wu, E.M. Tsai, BPIQ, a novel synthetic quinoline derivative, inhibits growth and induces mitochondrial apoptosis of lung cancer cells in vitro and in zebrafish xenograft model, BMC Cancer 15 (1) (2015) 962.
[20] M. Korcz, F. Sączewski, P. Bednarski, A. Kornicka, Synthesis, structure, chemical stability, and in vitro cytotoxic properties of novel quinoline-3-carbaldehyde hydrazones bearing a 1, 2, 4-triazole or benzotriazole moiety, Molecules 23 (6) (2018) 1497.
[21] Y.K. Al-Majedy, A.A.H. Kadhum, A.A. Al-Amiery, A.B. Mohamad, Coumarins: the antimicrobial agents, Sys. Rev. Pharm. 8 (1) (2017) 62–70.
[22] R.J. Naik, M.V. Kulkarni, K. Sreedhara Ranganath Pai, P.G. Nayak, Click chemistry approach for bis-chromenyl triazole hybrids and their antitubercular activity, Chem. Biol. Drug Des. 80 (4) (2012) 516–523.
[23] B.Z. Kurt, N.O. Kandas, A. Dag, F. Sonmez, M. Kucukislamoglu, Synthesis and biological evaluation of novel coumarin-chalcone derivatives containing urea moiety as potential anticancer agents, Arab J. Chem. (2017).
[24] G. Melagraki, A. Afantitis, O. Igglessi-Markopoulou, A. Detsi, M. Koufaki, C. Kontogiorgis, D.J. Hadjipavlou-Litina, Synthesis and evaluation of the antioxidant and anti-inflammatory activity of novel coumarin-3-aminoamides and their alpha-lipoic acid adducts, Eur. J. Med. Chem. 44 (7) (2009) 3020–3026.
[25] O.M. Abdelhafez, K.M. Amin, R.Z. Batran, T.J. Maher, S.A. Nada, S. Sethumadhavan, Synthesis, anticoagulant and PIVKA-II induced by new 4-hydroxycoumarin derivatives, Bioorg. Med. Chem. 18 (10) (2010) 3371–3378.
[26] J.Y. Yeh, M.S. Coumar, J.T. Horng, H.Y. Shiao, F.M. Kuo, H.L. Lee, I.C. Chen, C.W. Chang, W.F. Tang, S.N. Tseng, Anti-influenza drug discovery: structure–activity relationship and mechanistic insight into novel angelicin derivatives, J. Med. Chem. 53 (4) (2010) 1519–1533.
[27] D.H. Mahajan, C. Pannecouque, E. De Clercq, K.H. Chikhalia, Synthesis and Studies of New 2-(Coumarin-4-yloxy)-4, 6-(substituted)-s-Triazine Derivatives as Potential Anti-HIV Agents, Arch. Pharm. (Weinheim). 342 (5) (2009) 281–290.
[28] Y. Shokoohinia, L. Hosseinzadeh, M. Alipour, A. Mostafaie, H.-R. Mohammadi-Motlagh, Comparative evaluation of cytotoxic and apoptogenic effects of several coumarins on human cancer cell lines: osthole induces apoptosis in p53-deficient H1299 cells, Adv. Pharmacol. Sci. 2014 (2014) 847574.
[29] P.R. Kamath, D. Sunil, A.A. Ajees, K. Pai, S. Das, Some new indole–coumarin hybrids; Synthesis, anticancer and Bcl-2 docking studies, Bioorg. Chem. 63 (2015) 101–109.
[30] K. Thomas, A.V. Adhikari, I.H. Chowdhury, E. Sumesh, N.K. Pal, New quinolin-4-yl-1, 2, 3-triazoles carrying amides, sulphonamides and amidopiperazines as potential antitubercular agents, Eur. J. Med. Chem. 46 (6) (2011) 2503–2512.
[31] S. Manohar, A. Pepe, C.E.V. Gerena, B. Zayas, S.V. Malhotra, D.S. Rawat, Anticancer activity of 4-aminoquinoline-triazine based molecular hybrids, RSC Adv. 4 (14) (2014) 7062–7067.
[32] B. Ling, R. Zhang, Z. Wang, Y. Liu, C. Liu, Study on the interactions of smac mimetics with xiap-bir3 domain by docking and molecular dynamics simulations, J. Theor. Comput. Chem. 9 (04) (2010) 797–812.
[33] F. Cossu, E. Mastrangelo, M. Milani, G. Sorrentino, D. Lecis, D. Delia, L. Manzoni, P. Seneci, C. Scolastico, M. Bolognesi, Designing Smac-mimetics as antagonists of XIAP, cIAP1, and cIAP2, Biochem. Biophys. Res. Commun. 378 (2) (2009) 162–167.
[34] F. Xu, X. Gao, H. Li, S. Xu, X. Li, X. Hu, Z. Li, J. Xu, H. Hua, D. Li, Hydrogen sulfide releasing enmein-type diterpenoid derivatives as apoptosis inducers through mitochondria-related pathways, Bioorg. Chem. 82 (2019) 192–203.
[35] Y. Wang, C. Wu, Q. Zhang, Y. Shan, W. Gu, S. Wang, Design, synthesis and biological evaluation of novel β-pinene-based thiazole derivatives as potential anticancer agents via mitochondrial-mediated apoptosis pathway, Bioorg. Chem. 84 (2019) 468–477.
[36] Y. Shi, Mechanisms of caspase activation and inhibition during apoptosis, Mol. Cell 9 (3) (2002) 459–470.
[37] M. Ghasemian, M. Mahdavi, P. Zare, M.A.H. Feizi, Spiroquinazolinone-induced cytotoxicity and apoptosis in K562 human leukemia cells: alteration in expression levels of Bcl-2 and Bax, J. Toxicol. Sci. 40 (1) (2015) 115–126.
[38] P. Beale, P. Rogers, F. Boxall, S. Sharp, L. Kelland, BCL-2 family protein expression and platinum drug resistance in ovarian carcinoma, Br. J. Cancer 82 (2) (2000) 436–440.
[39] V.A. Barvaux, P. Lorigan, M. Ranson, A.M. Gillum, R.S. McElhinney, T.B.H. McMurry, G.P. Margison, Sensitization of a human ovarian cancer cell line to temozolomide by simultaneous attenuation of the Bcl-2 antiapoptotic protein and DNA repair by O6-alkylguanine-DNA alkyltransferase, Mol. Cancer Ther. 3 (10) (2004) 1215–1220.
[40] M. Mahdavi, M.M. Lavi, R. Yekta, M.A. Moosavi, M. Nobarani, S. Balalaei, S. Arami, M.R. Rashidi, Evaluation of the cytotoxic, apoptosis inducing activity and molecular docking of spiroquinazolinone benzamide derivatives in MCF-7 breast cancer cells, Chem. Biol. Interact. 260 (2016) 232–242.
[41] K. Engels, S. Knauer, D. Metzler, C. Simf, O. Struschka, C. Bier, W. Mann, A. Kovacs, R. Stauber, Dynamic intracellular survivin in oral squamous cell carcinoma: underlying molecular mechanism and potential as an early prognostic marker, J. Pathol. 211 (5) (2007) 532–540.
[42] I. Tamm, S. Richter, D. Oltersdorf, U. Creutzig, J. Harbott, F. Scholz, L. Karawajew, W.D. Ludwig, C. Wuchter, High expression levels of x-linked inhibitor of apoptosis protein and survivin correlate with poor overall survival in childhood de novo acute myeloid leukemia, Clin. Cancer Res. 10 (11) (2004) 3737–3744.
[43] A. Fassihi, K. Mahnam, B. Moeinifard, M. Bahmanziari, H.S. Aliabadi, A. Zarghi, R. Sabet, M. Salimi, M. Mansourian, Synthesis, calcium-channel blocking activity, and conformational analysis of some novel 1, 4-dihydropyridines: application of PM3 and DFT computational methods, Med. Chem. Res. 21 (10) (2012) 2749–2761.
[44] R.W. Armstrong, A.P. Combs, P.A. Tempest, S.D. Brown, T.A. Keating, Multiple-component condensation strategies for combinatorial library synthesis, Acc. Chem. Res. 29 (3) (1996) 123–131.
[45] A. Javid, S. Ahmadian, A. Saboury, S. Rezaei-Zarchi, Anticancer effect of doxorubicin loaded heparin based super-paramagnetic iron oxide nanoparticles against the human ovarian cancer cells, World Acad. Sci. Eng. Technol. 74 (2011) 143–149.
[46] E. Sattarinezhad, A.-K. Bordbar, N. Fani, Piperine derivatives as potential inhibitors of survivin: An in silico molecular docking, Comput. Biol. Med. 63 (2015) 219–227.
[47] I. Tamm, Y. Wang, E. Sausville, D.A. Scudiero, N. Vigna, T. Oltersdorf, J.C. Reed, IAP-family protein survivin inhibits caspase activity and apoptosis induced by Fas (CD95), Bax, caspases, and anticancer drugs, Cancer Res. 58 (23) (1998) 5315–5320.
[48] M. Mobahat, A. Narendran, K. Riabowol, Survivin as a preferential target for cancer therapy, Int. J. Mol. Sci. 15 (2) (2014) 2494–2516.
[49] S. Sakamoto, N. Kyprianou, Targeting anoikis resistance in prostate cancer metastasis, Mol. Aspects Med. 31 (2) (2010) 205–214.
[50] N. Takai, T. Ueda, M. Nishida, K. Nasu, I. Miyakawa, The relationship between oncogene expression and clinical outcome in endometrial carcinoma, Curr. Cancer Drug Targets 4 (6) (2004) 511–520.
[51] D.C. Altieri, Survivin, versatile modulation of cell division and apoptosis in cancer, Oncogene 22 (53) (2003) 8581–8589.
[52] X. Ling, R.J. Bernacki, M.G. Brattain, F. Li, Induction of survivin expression by taxol (paclitaxel) is an early event, which is independent of taxol-mediated G2/M arrest, J. Biol. Chem. 279 (15) (2004) 15196–15203.
[53] F. Pettersson, A. Dalgleish, R. Bissonnette, K. Colston, Retinoids cause apoptosis in pancreatic cancer cells via activation of RAR-γ and altered expression of Bcl-2/Bax, Br. J. Cancer 87 (5) (2002) 555–561.
[54] F. Tzifi, C. Economopoulou, D. Gourgiotis, A. Ardavanis, S. Papageorgiou, A. Scorilas, The role of BCL2 family of apoptosis regulator proteins in acute and chronic leukemias, Adv. Hematol. 2012 (2012) 524308.
[55] J. Plati, O. Bucur, R. Khosravi-Far, Apoptotic cell signaling in cancer progression and therapy, Integr. Biol. (Camb). 3 (4) (2011) 279–296.
[56] E. Tamanini, I.M. Buck, G. Chessari, E. Chiarparin, J.E. Day, M. Frederickson, C.M. Griffiths-Jones, K. Hearn, T.D. Heightman, A. Iqbal, Discovery of a Potent Non-peptidomimetic, Small-Molecule Antagonist of Cellular Inhibitor of Apoptosis Protein 1 (cIAP1) and X-linked Inhibitor of Apoptosis Protein (XIAP), J. Med. Chem. 60 (11) (2017) 4611–4625.
[57] V.P. Wadegaonkar, P.A. Wadegaonkar, Withanone as an inhibitor of survivin: A potential drug candidate for cancer therapy, J. Biotechnol. 168 (2) (2013) 229–233.
[58] M. Mansourian, K. Mahnam, A. Madadkar-Sobhani, A. Fassihi, L. Saghaie, Insights into the human A_1 adenosine receptor from molecular dynamics simulation: structural study in the presence of lipid membrane, Med. Chem. Res. 24 (10) (2015) 3645–3659.
[59] R.R. Nasab, M. Mansourian, F. Hassanzadeh, Synthesis, antimicrobial evaluation and docking studies of some novel quinazolinone Schiff base derivatives, Res. Pharm. Sci. 13 (3) (2018) 213–221.

[60] G.M. Morris, R. Huey, W. Lindstrom, M.F. Sanner, R.K. Belew, D.S. Goodsell, A.J. Olson, AutoDock4 and AutoDockTools4: Automated docking with selective receptor flexibility, J. Comput. Chem. 30 (16) (2009) 2785–2791.
[61] B. Ku, C. Liang, J.U. Jung, B.-H. Oh, Evidence that inhibition of BAX activation by BCL-2 involves its tight and preferential interaction with the BH3 domain of BAX, Cell Res. 21 (4) (2011) 627–641.
[62] L. Chantalat, D.A. Skoufias, J.-P. Kleman, B. Jung, O. Dideberg, R.L. Margolis, Crystal structure of human survivin reveals a bow tie–shaped dimer with two unusual α-helical extensions, Mol. Cell 6 (1) (2000) 183–189.
[63] G.M. Morris, D.S. Goodsell, R.S. Halliday, R. Huey, W.E. Hart, R.K. Belew, A.J. Olson, Automated docking using a Lamarckian genetic algorithm and an empirical binding free energy function, J. Comput. Chem. 19 (14) (1998) 1639–1662.
[64] A.C. Wallace, R.A. Laskowski, J.M. Thornton, LIGPLOT: a program to generate schematic diagrams of protein-ligand interactions, Protein Eng. Des. Sel. 8 (2) (1995) 127–134.